

Decentralized Federated Domain Generalization with Style Sharing: A Formal Modeling and Convergence Analysis

Shahryar Zehtabi^a, Dong-Jun Han^b, Seyyedali Hosseinalipour^c, Christopher G. Brinton^a

^a Purdue University, ^b Yonsei University, ^c University at Buffalo – SUNY

Abstract

Much of the federated learning (FL) literature focuses on settings where local dataset statistics remain the same between training and testing time. Recent advances in domain generalization (DG) aim to use data from source (training) domains to train a model that generalizes well to data from unseen target (testing) domains. In this paper, we are motivated by two major gaps in existing work on FL and DG: (1) the lack of formal mathematical analysis of DG objectives and training processes; and (2) DG research in FL being limited to the conventional star-topology architecture. Addressing the second gap, we develop *Decentralized Federated Domain Generalization with Style Sharing* (StyleDDG), a fully decentralized DG algorithm designed to allow devices in a peer-to-peer network to achieve DG based on sharing style information inferred from their datasets. Additionally, we fill the first gap by providing the first systematic approach to mathematically analyzing style-based DG training optimization. We cast existing centralized DG algorithms within our framework, and employ their formalisms to model StyleDDG. Based on this, we obtain analytical conditions under which a sub-linear convergence rate of StyleDDG can be obtained. Through experiments on two popular DG datasets, we demonstrate that StyleDDG can obtain significant improvements in accuracy across target domains with minimal added communication overhead compared to decentralized gradient methods that do not employ style sharing.

CCS Concepts

• **Computing methodologies** → *Cooperation and coordination; Distributed artificial intelligence.*

Keywords

Decentralized Federated Learning, Domain Generalization, Adaptive Instance Normalization

ACM Reference Format:

Shahryar Zehtabi^a, Dong-Jun Han^b, Seyyedali Hosseinalipour^c, Christopher G. Brinton^a. 2025. Decentralized Federated Domain Generalization with Style Sharing: A Formal Modeling and Convergence Analysis. In *Proceedings of 26th International Symposium on Theory, Algorithmic Foundations, and Protocol Design for Mobile Networks and Mobile Computing (MobiHoc '25)*. ACM, New York, NY, USA, 14 pages. <https://doi.org/XXXXXXX.XXXXXXX>

Permission to make digital or hard copies of all or part of this work for personal or classroom use is granted without fee provided that copies are not made or distributed for profit or commercial advantage and that copies bear this notice and the full citation on the first page. Copyrights for components of this work owned by others than the author(s) must be honored. Abstracting with credit is permitted. To copy otherwise, or republish, to post on servers or to redistribute to lists, requires prior specific permission and/or a fee. Request permissions from permissions@acm.org.

MobiHoc '25, Houston, TX

© 2025 Copyright held by the owner/author(s). Publication rights licensed to ACM.
ACM ISBN 978-1-4503-XXXX-X/2018/06
<https://doi.org/XXXXXXX.XXXXXXX>

1 Introduction

Federated learning (FL) enables multiple edge devices to collaboratively train a machine learning (ML) model using data stored locally on each device. Existing conventional “star-topology” FL methods rely on a central server to conventionally sent from the clients [26]. However, in decentralized networks, a central server may not always be available to conduct model aggregations [6]. Motivated by this, recent research has investigated decentralized federated learning (DFL), in which edge devices iteratively communicate their model parameters with their one-hop neighbors after completing their local model training [17]. While synchronization among the edge devices in conventional FL is readily guaranteed through the aggregation at the end of each training round, DFL algorithms need to incorporate a cooperative consensus strategy to their learning process so that devices gradually learn the same model [28].

When training ML models via FL, it is typically assumed that the test data is drawn from the same probability distribution as the training data [47]. However, this assumption does not always hold; in many real-world applications, a distribution shift can occur between the training set (source) and the test set (target) [4]. For example, consider an image classification task where the data-collecting devices can only capture images of objects during the morning and the afternoon (source domains), while our goal is to train a model which can also classify different objects in images taken at night (target domain). It has been shown that ML algorithms can drastically fail to achieve generalization to such unseen target domains without making any special adjustments to their training processes [36]. Domain generalization (DG) aims to mitigate this issue, with the goal of preventing a degradation in performance of ML models under such distribution shifts [47].

Due to the practical importance of enabling DG in FL settings, recent research has focused on federated domain generalization (FDG) [2], where DG algorithms are designed to operate in a distributed manner across edge devices. FDG introduces further challenges compared to centralized DG, primarily due to the limited number of source domains accessible to each device [24]. In FDG, in addition to label heterogeneity across devices, source heterogeneity must be also considered, further complicating the goal of achieving DG [37]. For instance, in the previously mentioned example, one device may contain images collected in the morning, while another holds images taken in the afternoon, yet the constructed global model is expected to make reliable predictions on night-time images.

Research Objectives: A large class of DG algorithms are *style-based*, with style statistics estimated from the source dataset and explored for generalization to the target. These works, whether for centralized training [47] or star-topology FL [2], lack a concrete mathematical formulation of the objective function being optimized to train domain-invariant models. Furthermore, the studied DG algorithms in FL are constrained by their star-topology networks, and

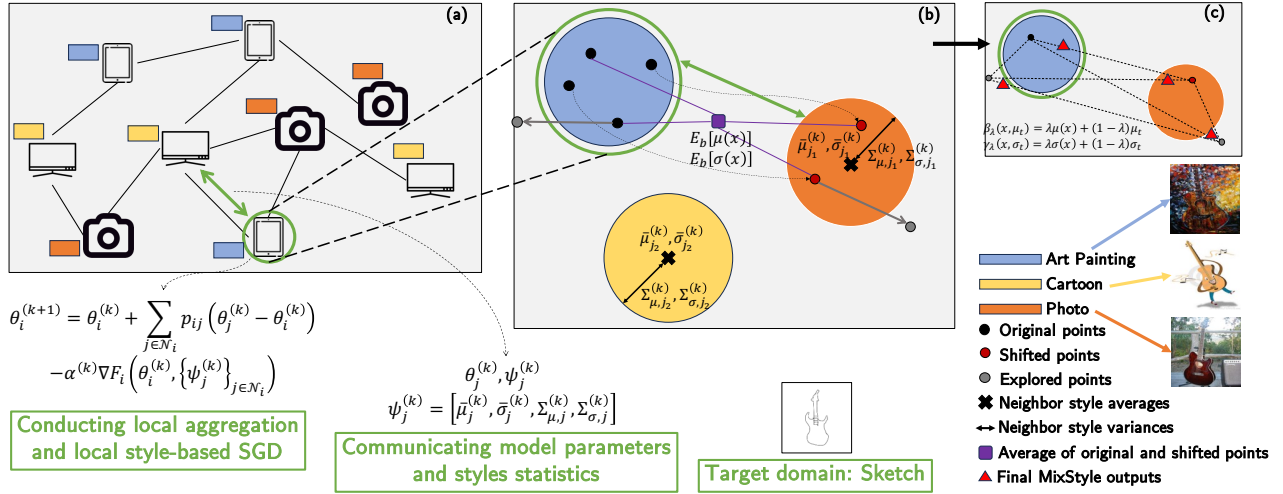


Figure 1: System model and visualization of proposed DDG methodology. (a) A decentralized network comprised of $m = 9$ devices, with each device having data from one of three domains (art painting, cartoon, photo). The performance of DDG is evaluated on the fourth domain (sketch). (b) In StyleDDG, each device first uses the style statistics of a neighbor for style shifting (getting to red dots from the black ones) for half its batch size. Then it concatenates the original plus the shifted points and chooses half of them to do style extrapolation with and generate new styles (grey dots). The circles shown here are illustrations of the style space at the output of a neural network layer. (c) After randomly shifting half of the points in the original mini-batch to a new style, and then randomly extrapolating half of the outputs, we are left with a new set of styles with size equal to the original mini-batch. In StyleDDG, we use these new points (red triangles) and apply MixStyle within them.

cannot be readily extended to arbitrary decentralized networks. In this paper, we present one of the first style-based decentralized FDG algorithms, called *Decentralized Federated Domain Generalization with Style Sharing* (StyleDDG), in which edge devices communicate style information of their local datasets with their one-hop neighbors so that collectively they can train ML models that generalize well to unseen domains. Our StyleDDG algorithm, illustrated in Fig. 1, is inspired by the work in [31], where the authors present an FDG algorithm called StableFDG. Different than [31], StyleDDG is a fully decentralized DG algorithm, and does not add any further oversampling or attention layers as in StableFDG. The computation overhead of StableFDG is at least doubled compared to its analogous models, due to its oversampling step and the added attention layer, and this in turn obstructs our understanding of its style exploration strategy in achieving DG performance. Lastly, our other main contribution is to provide the first formal modeling of style-based DG training, both for well-known DG methods and for StyleDDG.

Contributions: Our key contributions are as follows:

- We present StyleDDG, one of the first fully decentralized domain generalization (DDG) algorithms. In our problem setup, devices in a decentralized system aim to achieve DG without having any information about the whole network graph, and can only communicate with their one-hop neighbors, unlike in star-topology FL. Specifically, each device in DDG trains an ML model locally using its local dataset, and then it exchanges (i) its ML model parameters and (ii) style statistics of its current batch with its neighbors (see Fig. 1-(a)). Afterward, each device employs the received style statistics from its neighbors to explore the style space more effectively for DG (see Fig. 1-(b)).
- Among all style-based DG methods, for the first time in the literature, we provide a systematic approach to mathematically

formulate the training objective function and optimization procedure. As the operations of style-based methods have commonalities, we first derive a set of concrete formulations for well-known style-based DG methods. These generalized formulations lay the groundwork for formal modeling of future methods in this emerging field, applicable to both centralized and distributed/federated network settings.

- Following the above-mentioned analytical framework, we present a formal modeling of the objective function of StyleDDG. Exploiting this rigorous formulation, we conduct convergence analysis on our methodology, enabling us to provide one of the first convergence guarantees among all style-based DG papers. Our results illustrate that under certain conditions on the employed ML model, the smoothness of local loss functions can be guaranteed for each device. Consequently, this ensures that all devices collectively converge to the same optimal model.
- Through experiments on two DG datasets, we demonstrate that our StyleDDG method outperforms other centralized/federated DG methods applied in a decentralized learning setting, in terms of the final achievable test accuracy on unseen target domains.

2 Related Work

Decentralized Federated Learning (DFL). A recent line of work has considered FL over non-star topologies. This includes semi-decentralized FL [8, 30], which groups the devices into several subnetworks, with devices conducting intra-subnet communications before exchanging their model parameters with the centralized server. Fog learning generalizes this to multi-layer hierarchies between the edge devices and the backbone servers [12].

DFL is at the extreme end of this spectrum, where communication is entirely peer-to-peer, with the goal of iteratively updating and exchanging models over the device graph to arrive at an optimal ML model [25, 27, 44]. Optimization of DFL has been studied

in e.g., [46], in which a gradient tracking method for DFL is developed, and [14], which proposed designing overlays on top of the physical network graph. Literature on decentralized optimization of non-convex loss functions, including Decentralized SGD [17] and DSpodFL [43], have provided theoretical guarantees on DFL convergence behavior. Nevertheless, currently there does not exist any DFL algorithm which is tailored for DG. In this paper, we propose a DG methodology tailored to the DFL network setting, leading to one of the first style-based DDG algorithms in the literature.

Domain Generalization (DG). DG aims to achieve generalization to out-of-distribution data from unseen target domains using distinct source domain data for training (see [36, 47] for recent surveys). While various classes of ML methods can be considered DG – like meta-learning [3, 18], self-supervised learning [7], regularization [15] and domain alignment [10, 20] – our focus in this paper is on the family of *feature augmentation, style-based* methods for DG. In particular, algorithms like MixStyle [49] and DSU [22] achieve DG via feature-level augmentation, where the styles of images are explored beyond the distribution of styles that exist within the source domains. In the core of these algorithms, they employ AdaIN [13] (adaptive instance normalization) to explore new features/styles during training. Compared to other DG methods, an advantage of style-based methods is that they do not require the domain labels to be known [31].

Despite the notable progress in this domain, a major drawback of current research on DG is the lack of concrete formulations for objective functions. Thus, convergence guarantees for these methods have remained elusive. In this paper, we rigorously formulate the optimization procedures of prior well-known DG methods and our methodology in a concrete and compact fashion, which enables us to conduct convergence analysis on our methodology. Our theoretical contributions in this paper thus open the door for the formulation and convergence analysis of future DG methods.

Federated Domain Generalization (FDG). Data heterogeneity is a notable challenge in FL, as the distribution of data among devices are non-IID [21]. This challenge becomes even more prominent when the distribution of test data is different than the distribution of training data available in devices, motivating the development of FDG algorithms. In this direction, FedBN [23] proposed to not average the local batch normalization layers to alleviate the feature shift problem. In COPA [38], each device uses hybrid batch-instance normalization to learn domain-invariant models, In FedSR [29], each device employs an L2-norm regularizer and a conditional mutual information regularizer on the representations to guide the model to only learn essential domain-invariant information. In CCST [9], each device uses a VGG encoder to extract style information of images during training. In StableFDG [31], each device uses one of the styles of other devices received from the server, and extrapolates the region outside the existing style domains to achieve generalization.

However, these existing FDG methods are tailored for conventional star-topology FL settings. Decentralized FL introduces novel challenges due to the need to incorporate peer-to-peer consensus mechanisms. In this paper, we present one of the first decentralized domain generalization (DDG) algorithms. Furthermore, we are unaware of any style-based DG algorithm with concrete convergence

analysis. Our work thus fills an important gap through our formal modeling of the DG objective functions, which not only helps us gain insights to the theoretical implications of our proposed methodology, but also lays the foundation for rigorous formulation and convergence analysis of future style-based DG methods.

3 Style-Based Domain Generalization

We begin with a set of notations and preliminary definitions in Sec. 3.1. Then in Sec. 3.2 we discuss the problem formulation. Finally, we provide a novel mathematical formulation for the objective functions of two centralized DG algorithms in Sec. 3.3, which will be later used in Sec. 4 to formulate our novel StyleDDG algorithm.

3.1 Preliminaries

3.1.1 Notation. We denote the model parameters of a neural network with dimension $n \in \mathbb{Z}^+$ by $\theta \in \mathbb{R}^n$. For DG methods over vision/image applications, usually convolutional neural networks (CNNs) are used, which consist of multiple convolutional blocks. Let us partition the model θ to $L \in \mathbb{Z}^+$ partitions. We use the notation $\theta_\ell \subset \theta$ with $\ell = 1, \dots, L$ as the sub-model with the model parameters of only partition ℓ of the model θ . Thus, we will have $\theta = [\theta_1^T \ \dots \ \theta_L^T]^T$. For example, we can partition a ResNet model [11] by some of its convolutional layers/blocks (See Fig. 2-(b)).

We abstract the operations applied at the end of each layer ℓ as $h_{\theta_\ell}(\cdot)$, making the final output of the CNN for an input x be given as $(h_{\theta_L} \circ \dots \circ h_{\theta_1})(x)$ where \circ denotes the composition operator of two functions. Let us denote the loss function as $\mathcal{L}(h_\theta(x), y)$ which takes the predicted outputs $h_\theta(x)$ and true labels y and calculates the loss based on them. Also, let $\hat{\mathcal{P}}(\cdot)$ denote the power set of a given set. We define a function \mathcal{P} which takes a positive integer input $L \in \mathbb{Z}^+$ and outputs $\mathcal{P}(L) = \hat{\mathcal{P}}(\{\ell : 1 \leq \ell \leq L\})$. We note that the cardinality of this function for a given L is $|\mathcal{P}(L)| = 2^L$. Finally, let $\mathcal{S}_{\mathcal{I}}$ be the set of all possible permutations of the set \mathcal{I} .

3.1.2 AdaIN. Adaptive instance normalization (AdaIN) [13] plays a key role in style-based DG methods by enabling style transfers. This technique removes the style information of a data sample and replaces it with the style of another sample. Specifically, the AdaIN process can be written as follows:

$$\text{AdaIN}(x, \mu_t, \sigma_t) = \sigma_t \frac{x - \mu(x)}{\sigma(x)} + \mu_t, \quad (1)$$

where the tensor $x \in \mathbb{R}^{B \times C \times H \times W}$ is taken to be a batch of size B at a specific layer of the CNN with a channel dimension of C , width W and height H , where $x_{b,c,h,w}$ denotes the value at the indexed dimensions. Furthermore, $\mu_t, \sigma_t \in \mathbb{R}^{B \times C}$ are the statistics of a target style to which we want to shift the style of x to, and the instance-level mean and standard deviation $\mu(x), \sigma(x) \in \mathbb{R}^{B \times C}$ for each channel are calculated as

$$\begin{aligned} \mu(x)_{b,c} &= \frac{1}{HW} \sum_{h=1}^H \sum_{w=1}^W x_{b,c,h,w}, \\ \sigma^2(x)_{b,c} &= \frac{1}{HW} \sum_{h=1}^H \sum_{w=1}^W (x_{b,c,h,w} - \mu(x)_{b,c})^2, \end{aligned} \quad (2)$$

where $\mu(x) = [\mu(x)_{b,c}]_{\substack{1 \leq b \leq B \\ 1 \leq c \leq C}}$ and $\sigma(x) = [\sigma(x)_{b,c}]_{\substack{1 \leq b \leq B \\ 1 \leq c \leq C}}$. We note that the AdaIN function in Eq. (1) first normalizes the style of x by

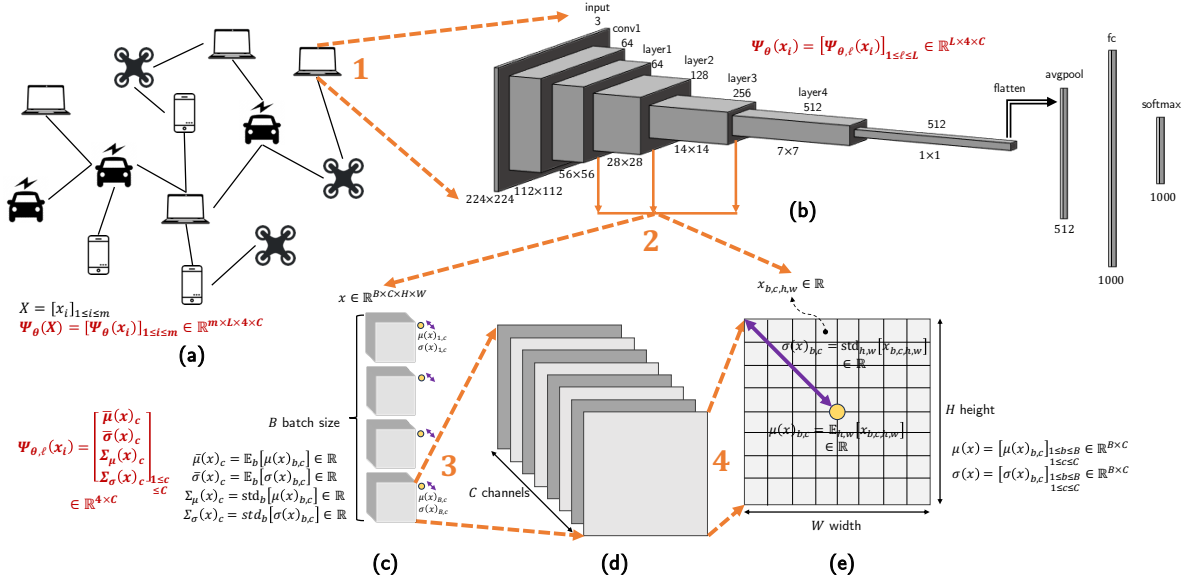


Figure 2: Illustration the style statistics used in our paper. (a) A decentralized network with heterogeneous devices having access to data from only a single domain. (b) An overview of the ResNet18 model [11] is shown as an example of the model at each device, where the number of channels are written above the blocks, and the output size is written below them. We visualize the blocks/layers that StyleDDG is applied to, which correspond to layers where we extract style statistics from. (c) Illustrates the outputs of a particular layer for all instances in the batch of size B . The style statistics that each device shares with its neighbors are obtained in the batch-level as shown. (d) For a given instance in the batch, the style statistics are calculated for each channel separately. (e) Finally, this subfigure demonstrates how the μ and σ of style statistics are computed based on the mean and standard deviation of the layer output values.

calculating $(x - \mu(x))/\sigma(x)$, and then scales the result by σ_t and shifts it by μ_t to move it to a desired target style.

3.1.3 Higher-order statistics. After computing the mean $\mu(x)$ and standard deviation $\sigma(x)$ for a given batch x as its first-order style statistics, we can further extract second-order style statistics denoted by $\Sigma_\mu^2(x), \Sigma_\sigma^2(x) \in \mathbb{R}^C$ as the variance of each of them as

$$\begin{aligned} \Sigma_\mu^2(x)_c &= \frac{1}{B} \sum_{b=1}^B (\mu(x)_{b,c} - \mathbb{E}_b[\mu(x)_{b,c}])^2, \\ \Sigma_\sigma^2(x)_c &= \frac{1}{B} \sum_{b=1}^B (\sigma(x)_{b,c} - \mathbb{E}_b[\sigma(x)_{b,c}])^2, \end{aligned} \quad (3)$$

where $\Sigma_\mu^2(x) = [\Sigma_\mu^2(x)_c]_{1 \leq c \leq C}$ and $\Sigma_\sigma^2(x) = [\Sigma_\sigma^2(x)_c]_{1 \leq c \leq C}$.

3.2 Problem Formulation

We consider a decentralized FL network represented by a graph $\mathcal{G} = (\mathcal{M}, \mathcal{E})$, where $\mathcal{M} = \{1, \dots, m\}$ is the set of devices/nodes, and \mathcal{E} indicates the set of communication edges between the devices. We assume that the graph is connected, and define the set of one-hop neighbors of a device $i \in \mathcal{M}$ as \mathcal{N}_i . Each device i maintains an ML model θ_i , and engages in local computations and inter-device communications to train a globally optimal model. Also, each device i contains a local dataset $\mathcal{D}_i = \{(x_i, y_i, d_i)_k\}_{k=1}^{|\mathcal{D}_i|}$ where the $(x_i, y_i, d_i)_k$ pair indicates the k th data point with input features x_i , label y_i , and domain d_i . For example, in the well-known PACS dataset [19], each domain corresponds to a visual style, namely, art painting, cartoon, photo, or sketch.

In our DGD setting, the goal is to train a domain-invariant global model that generalizes well to unseen domains. In the PACS dataset

example, a global model trained on art painting, cartoon, and photo domains should generalize well to the sketch domain, despite the absence of sketch data during the model training process.

3.3 Formal Modeling of Centralized Algorithms

In this section, we provide mathematical modeling of the MixStyle [49] and DSU [22] algorithms for centralized DG. Note that the original papers and subsequent works do not present any such objective functions. We will later use the ideas and functions developed here when presenting our own StyleDDG algorithm in Sec. 4.2.

3.3.1 MixStyle [49]. In MixStyle, the style space of the CNN layers are explored through convex combinations of the existing styles, thereby exposing the model to styles beyond the existing ones in the training batch. For a given instance x and target style statistics μ_t and σ_t , the MixStyle operation uses AdaIN from Eq. (1) as

$$\text{MixStyle}_\lambda(x, \mu_t, \sigma_t) = \text{AdaIN}(x, \beta_\lambda(x, \mu_t), \gamma_\lambda(x, \sigma_t)), \quad (4)$$

where the shifting and scaling parameters are defined as

$$\begin{aligned} \beta_\lambda(x, \mu_t) &= \lambda\mu(x) + (1 - \lambda)\mu_t, \\ \gamma_\lambda(x, \sigma_t) &= \lambda\sigma(x) + (1 - \lambda)\sigma_t, \end{aligned} \quad (5)$$

respectively, and λ is the mixing coefficient. The original paper [49] applies MixStyle to all convolutional blocks except the last one for ResNet ($L = 3$). Letting \mathbb{P}_λ be the probability distribution which the mixing coefficient λ for each layer are sampled from, [49] models $\mathbb{P}_\lambda = \text{Beta}(0.1, 0.1)$ as the Beta distribution and the probabilities $p_\ell = 0.5$ for all the layers $\ell = 1, \dots, L$, where p_ℓ is the probability of applying MixStyle to layer ℓ .

Our formal objective model. We can now formally model MixStyle's objective function. For a mini-batch x of size B , MixStyle's

loss function with random shuffling can be expressed as

$$F(\theta) = \sum_{\pi \in \mathcal{P}(L)} \left(\prod_{\ell \in \pi} p_\ell \right) \mathbb{E}_{\substack{(x,y) \sim \mathbb{P}_D \\ \{I_\ell \in \mathfrak{S}_B\}_{\ell \in \pi} \\ \{\lambda_\ell \sim \mathbb{P}_\lambda\}_{\ell \in \pi}}} \left[\mathcal{L}(\hat{h}_{\theta, \{I_\ell, \lambda_\ell\}_{\ell \in \pi}}(x), y) \right], \quad (6)$$

where \mathbb{P}_D denotes the probability distribution of data in the source domains and \mathfrak{S}_B is the set of all possible permutations of the set $B = \{1, \dots, B\}$. What this method essentially does is apply its MixStyle strategy to the outputs of the model's layer ℓ with a probability p_ℓ , so that the overall model is modified as

$$\hat{h}_{\theta, \{I_\ell, \lambda_\ell\}_{\ell \in \pi}}(x) = (\hat{h}_{\theta_L, I_L, \lambda_L} \circ \dots \circ \hat{h}_{\theta_1, I_1, \lambda_1})(x), \quad (7)$$

in which $\hat{h}_{\theta_\ell, I_\ell, \lambda_\ell} = h_{\theta_\ell}$ if $\ell \notin \pi$. If $\ell \in \pi$, we define $x_m = [x_k]_{k \in I_\ell}^T$ as a permuted version of the mini-batch x based on the shuffled indices I_ℓ , and then the MixStyle update that occurs at that layer can be defined using Eq. (4) as

$$\hat{h}_{\theta_\ell, I_\ell, \lambda_\ell}(x) = \text{MixStyle}_{\lambda_\ell}(h_{\theta_\ell}(x), \mu(h_{\theta_\ell}(x_m)), \sigma(h_{\theta_\ell}(x_m))). \quad (8)$$

Note that the MixStyle layer is taking the model outputs for mini-batch x and the style statistics $\mu(\cdot)$ and $\sigma(\cdot)$ of the permuted mini-batch x_m calculated by Eq. (2) to do feature augmentation.

3.3.2 DSU [22]. DSU is another centralized DG algorithm where the style space of the CNN layers are explored by adding a Gaussian noise to the existing styles. For a given instance x and target higher-order style statistics $\Sigma_{\mu, t}$ and $\Sigma_{\sigma, t}$, the DSU operation invokes AdaIN from Eq. (1) as

$$\text{DSU}_{\epsilon_\mu, \epsilon_\sigma}(x, \Sigma_{\mu, t}, \Sigma_{\sigma, t}) = \text{AdaIN}(x, \beta_{\epsilon_\mu}(\mu(x), \Sigma_{\mu, t}), \gamma_{\epsilon_\sigma}(\sigma(x), \Sigma_{\sigma, t})), \quad (9)$$

where the shifting and scaling parameters are defined as

$$\beta_{\epsilon_\mu}(\mu, \Sigma_{\mu, t}) = \mu + \epsilon_\mu \Sigma_{\mu, t}, \quad \gamma_{\epsilon_\sigma}(\sigma, \Sigma_{\sigma, t}) = \sigma + \epsilon_\sigma \Sigma_{\sigma, t}, \quad (10)$$

respectively, and ϵ_μ and ϵ_σ follow a Normal distribution. Specifically, [22] applies DSU to all convolutional blocks alongside the first convolutional layer and the max pooling layer of a ResNet model ($L = 6$). Letting $\mathbb{P}_{\epsilon_\mu}, \mathbb{P}_{\epsilon_\sigma}$ be the probability distribution from which the exploration coefficients $\epsilon_{\mu, \ell}, \epsilon_{\sigma, \ell}$ are sampled for each layer ℓ , it sets the distributions $\mathbb{P}_{\epsilon_\mu} = \mathbb{P}_{\epsilon_\sigma} = \mathcal{N}(0, 1)$ as the unit Gaussian and the probabilities $p_\ell = 0.5$ for all layers $\ell = 1, \dots, L$.

Our formal objective model. For a mini-batch x of size B , we formalize the loss function of DSU as

$$F(\theta) = \sum_{\pi \in \mathcal{P}(L)} \left(\prod_{\ell \in \pi} p_\ell \right) \mathbb{E}_{\substack{(x,y) \sim \mathbb{P}_D \\ \{\epsilon_{\mu, \ell} \sim \mathbb{P}_{\epsilon_\mu}\}_{\ell \in \pi} \\ \{\epsilon_{\sigma, \ell} \sim \mathbb{P}_{\epsilon_\sigma}\}_{\ell \in \pi}}} \left[\mathcal{L}(\hat{h}_{\theta, \{\epsilon_{\mu, \ell}, \epsilon_{\sigma, \ell}\}_{\ell \in \pi}}(x), y) \right]. \quad (11)$$

In essence, this method applies its DSU strategy to the outputs of the model's layer ℓ with a probability p_ℓ , so that the overall model is modified as

$$\hat{h}_{\theta, \{\epsilon_{\mu, \ell}, \epsilon_{\sigma, \ell}\}_{\ell \in \pi}}(x) = (\hat{h}_{\theta_L, \epsilon_{\mu, L}, \epsilon_{\sigma, L}} \circ \dots \circ \hat{h}_{\theta_1, \epsilon_{\mu, 1}, \epsilon_{\sigma, 1}})(x), \quad (12)$$

in which $\hat{h}_{\theta_\ell, \epsilon_{\mu, \ell}, \epsilon_{\sigma, \ell}} = h_{\theta_\ell}$ if $\ell \notin \pi$. If $\ell \in \pi$, then the DSU update that occurs at that layer can be defined as

$$\hat{h}_{\theta_\ell, \epsilon_{\mu, \ell}, \epsilon_{\sigma, \ell}}(x) = \text{DSU}_{\epsilon_{\mu, \ell}, \epsilon_{\sigma, \ell}}(h_{\theta_\ell}(x), \Sigma_\mu(h_{\theta_\ell}(x)), \Sigma_\sigma(h_{\theta_\ell}(x))), \quad (13)$$

where the DSU layer takes the model outputs for mini-batch x and the higher-order style statistics $\Sigma_\mu(\cdot)$ and $\Sigma_\sigma(\cdot)$ of that batch as calculated in Eq. (3) to conduct feature augmentation.

The loss function formulations we derived in Eqs. (6) and (11) provide us with compact representations that will enable us to formally model our StyleDDG algorithm in Sec. 4. We observe that minimizing Eqs. (6) and (11) results in learning style-invariant model parameters for all different combinations of the layers/blocks in the CNN, by taking a convex combination of the styles (for MixStyle) and adding Gaussian noise to the styles of each layer (for DSU).

4 Decentralized Style-Based DG

In this section, we first present the steps of our StyleDDG algorithm in Sec. 4.1. Enabled by our formulations of the objective functions of the centralized algorithms in Sec. 3.3, we proceed to formally model StyleDDG in Sec. 4.2.

4.1 Algorithm

4.1.1 Gradient Descent and Consensus Mechanism. In our decentralized setup of interest, each device $i \in \mathcal{M}$ maintains a unique model $\theta_i^{(k)}$ at each iteration k of the training process. A consensus mechanism is necessary to ensure $\lim_{k \rightarrow \infty} \theta_1^{(k)} = \dots = \lim_{k \rightarrow \infty} \theta_m^{(k)}$. To this end, we represent the update rule for each device $i \in \mathcal{M}$ at each iteration k as

$$\theta_i^{(k+1)} = \theta_i^{(k)} + \sum_{j \in \mathcal{N}_i} p_{ij} \left(\theta_j^{(k)} - \theta_i^{(k)} \right) - \alpha^{(k)} g_i^{(k)}, \quad (14)$$

in which p_{ij} is a mixing coefficient used for the model parameters of device pair (i, j) , where we employ the commonly used Metropolis-Hastings weights $p_{ij} = \min\{1/(1 + |\mathcal{N}_i|), 1/(1 + |\mathcal{N}_j|)\}$ [40]. Furthermore, $g_i^{(k)} = \nabla F_i(\theta_i^{(k)}, [\psi_j^{(k)}]_{j \in \mathcal{N}_i})$ is the style-based gradient of device $i \in \mathcal{M}$ at iteration k obtained based on the local loss function, which will be elaborated in Sec. 4.1.3.

In a nutshell, the novelty of our algorithm is two-fold: (i) StyleDDG is, to our knowledge, the first fully decentralized style-based algorithm for DG, where the consensus-based decentralized update rule in Eq. (14) is used with modified gradients $\nabla F_i(\theta_i^{(k)}, [\psi_j^{(k)}]_{j \in \mathcal{N}_i})$ to achieve DG; and (ii) our style-based approach utilizes style information sharing only between the one-hop neighbors of a device $i \in \mathcal{M}$ to train style-invariant ML models.

The pseudo-code given in Alg. 1 outlines the steps of our StyleDDG method for all devices. Also, Fig. 3 showcases the pipeline of operations at each device $i \in \mathcal{M}$.

4.1.2 Style Statistics. Let $X \in \mathbb{R}^{m \times B}$ be the concatenation of all local mini-batches of data from the devices, i.e., $X = [x_1 \dots x_m]^T$. We denote the set of styles from all devices obtained using model parameters θ and combined batch X for all devices as $\Psi_\theta(X) = [\psi_\theta(x_1) \dots \psi_\theta(x_m)]^T$. The style tensor that each device $i \in \mathcal{M}$ calculates and shares with its neighbors is defined as $\psi_\theta(x_i) = [\psi_{\theta, 1}(x_i) \dots \psi_{\theta, L}(x_i)]^T$, which is obtained for different layers/blocks of the CNN model. Each individual style in this tensor consists of four style statistics at each layer/block $\psi_{\theta, \ell}(x_i) =$

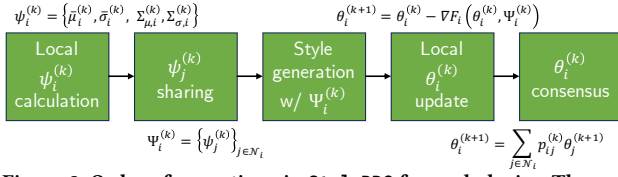


Figure 3: Order of operations in StyleDDG for each device. There are two steps of communication among the devices at each iteration of training, one for style sharing and another for model consensus. This is to ensure that up-to-date style statistics are being used.

$$\begin{aligned} & \left[\bar{\mu}_{\theta,\ell}(x_i) \quad \bar{\sigma}_{\theta,\ell}(x_i) \quad \Sigma_{\mu,\theta,\ell}^2(x_i) \quad \Sigma_{\sigma,\theta,\ell}^2(x_i) \right]^T \text{ derived as follows} \\ \bar{\mu}_{\theta,\ell}(x_i)_c &= \frac{1}{B} \sum_{b=1}^B \mu(h_{\theta,\ell}(x_i))_{b,c}, \quad \bar{\sigma}_{\theta,\ell}(x_i)_c = \frac{1}{B} \sum_{b=1}^B \sigma(h_{\theta,\ell}(x_i))_{b,c}, \\ \Sigma_{\mu,\theta,\ell}^2(x_i)_c &= \Sigma_{\mu}^2(h_{\theta,\ell}(x_i))_c, \quad \Sigma_{\sigma,\theta,\ell}^2(x_i)_c = \Sigma_{\sigma}^2(h_{\theta,\ell}(x_i))_c, \end{aligned} \quad (15)$$

where the definition of the functions $\mu(\cdot)_{b,c}$ and $\sigma(\cdot)_{b,c}$ were given in Eq. (2), and the definitions of $\Sigma_{\mu}^2(\cdot)_c$ and $\Sigma_{\sigma}^2(\cdot)_c$ in Eq. (3).

Therefore, the dimensions of the style vectors will be $\psi_{\theta,\ell}(x_i) \in \mathbb{R}^{L \times 4 \times C}$ for each layer, $\psi_{\theta,\ell}(x_i) \in \mathbb{R}^{L \times 4 \times C}$ for each device and $\Psi_{\theta,\ell}(X) \in \mathbb{R}^{m \times L \times 4 \times C}$ for the whole network. See Fig. 2 for a detailed illustration of the above-mentioned style vectors and style statistics.

REMARK 4.1. (Communication overhead) The added communication overhead for sharing the style statistics $\psi_{\theta,\ell}(x_i) \in \mathbb{R}^{L \times 4 \times C}$ is negligible relative to the model parameters $\theta \in \mathbb{R}^n$. Take the ResNet18 CNN model as an example, with around $n = 11.69$ million parameters. The number of parameters in the full style statistics vector in StyleDDG will be 1792 (since there are four equidimensional style statistics at each layer, and they are calculated in the outputs of the first three convolutional blocks with channel numbers 64, 128 and 256, respectively). As a result, the added communication overhead is 0.015%, which is negligible.

4.1.3 Style Exploration Strategy. In StyleDDG, the goal of each device is to communicate style information with its neighbors, so that they can collectively train domain-invariant models. Towards this, we apply three functions to the outputs of particular layers of a CNN, namely, StyleShift, StyleExplore and MixStyle. In the following subsections, we explain the details of each of them.

StyleShift. Each client first shifts the styles of half of a mini-batch at a particular layer to the styles received from a neighbor. This is illustrated in Fig. 1-(b), and we call it the StyleShift layer. In a generic definition, StyleShift takes the the batch $x = [x_s \quad x_s^c]$ which has already been separated to two equal-size parts x_s and x_s^c , and used the style vector ψ to shift the styles of half of it as

$$\text{StyleShift}_{\psi, \epsilon_{\mu}, \epsilon_{\sigma}}(x_s, x_s^c) = [\tilde{x}_s \quad x_s^c]^T, \quad (16)$$

where

$$\tilde{x}_s = \text{AdaIN}(x_s, \beta_{\epsilon_{\mu}, \ell}(\mathbf{1}_{B/2} \bar{\mu}_{j,\ell}^T, \Sigma_{\mu,j,\ell}), \gamma_{\epsilon_{\sigma}, \ell}(\mathbf{1}_{B/2} \bar{\sigma}_{j,\ell}^T, \Sigma_{\sigma,j,\ell})), \quad (17)$$

where $\mathbf{1}_{B/2}$ is an all-ones vector of size $B/2$, and the batch size B is chosen to be a multiple of 2. Also, the definition of AdaIN function was given in Eq. (1), and the shifting and scaling hyperparameters are the same ones used for DSU as defined in Eq. (10).

StyleExplore. After shifting the styles of half the points, we perform a subsequent step called *style exploration*, to further expand

the style space each device is exposed to during training. To this end, we first calculate intra-device average of style statistics, i.e., $\mathbb{E}_b[\mu(x)]$ and $\mathbb{E}_b[\sigma(x)]$, which are also illustrated in Fig. 1-(b). Then, we use those average points to extrapolate half of StyleShift outputs outwards of the style space, as illustrated in Fig. 1-(b). To mathematically model the points being extrapolated, we let the StyleExplore function take a 0-1 vector I_e as input, with the number of 0s being equal to 1s, and shift those points in x which correspond to 1s in I_e . In other words, for a general given vector x , we choose half of it $x_e = [x_k]_{k \in \{1, \dots, B\}; (I_e)_k=1}^T$ to apply style extrapolation on and keep the rest $x_e^c = [x_k]_{k \in \{1, \dots, B\}; (I_e)_k=1}^T$ the same. We finally concatenate them to get

$$\begin{aligned} \mu_e &= \begin{bmatrix} \mu(x_e) + \alpha(\mu(x_e) - \mathbb{E}_b[\mu(x)]) \\ \mu(x_e^c) \end{bmatrix}, \\ \sigma_e &= \begin{bmatrix} \sigma(x_e) + \alpha(\sigma(x_e) - \mathbb{E}_b[\sigma(x)]) \\ \sigma(x_e^c) \end{bmatrix}, \end{aligned} \quad (18)$$

where α is an exploration hyperparameter, and is set to $\alpha = 3$ (similar to [31]). Different that [31], we do not do any oversampling in this layer to avoid doubling the computation overhead of our methodology. This is a very critical modification to make, since other well-known DG methods such as [22, 23, 49] all operate with the rationale that style exploration layers should be plug-and-play components of existing models.

MixStyle. In the end, we use another set of indices I_m (a 0-1 vector similar to I_e) to obtain a permutation of μ_e and σ_e of Eq. (18) and use them to do MixStyle. The MixStyle functions was given in Eq. (4), and this step of our method is also illustrated in Fig. 1-(c). The finalized function can be written as

$$\text{StyleExplore}_{\lambda, I_e, I_m}(x) = \text{MixStyle}_{\lambda} \left(x, [\mu_e]_{k \in I_m}^T, [\sigma_e]_{k \in I_m}^T \right). \quad (19)$$

4.2 Formal Modeling of StyleDDG

In this section, we provide a formal modeling of StyleDDG. Since our goal is to analyze the performance of all devices in the decentralized setup, we break the loss function to a global loss and a device-side local loss. This leads to one of the first concrete formulations among all style-based DG papers (centralized and federated algorithms included), with compact representations of both the global and loss functions. We will later exploit our modeling in the convergence analysis of our methodology in Sec. 5.

4.2.1 Global Loss. Given a set of devices $\mathcal{M} = \{1, \dots, m\}$, the global loss function of StyleDDG can be formulated as

$$F(\theta) = \frac{1}{m} \sum_{i=1}^m \mathbb{E}_{\{(x_j, y_j) \sim \mathcal{P}_{D_j}\}_{j \in \mathcal{M}}} [F_i(\theta, \Psi_{\theta,i}(X))], \quad (20)$$

where $F_i(\theta, \Psi_{\theta,i}(X))$ is the local loss function of each device $i \in \mathcal{M}$ evaluated with given model parameters θ and combined batch X for all devices, in which $\Psi_{\theta,i}(X) \subset \Psi_{\theta}(X)$ is the set of styles from the neighbors of device i . Note that in Eq. (20), if instead of $\Psi_{\theta,i}(X)$ we input the full style information of all devices $\Psi_{\theta}(X)$ to each individual device, we obtain the loss function that StableFDG [31] aims to minimize in the conventional star-topology FL setup.

Algorithm 1: Decentralized Domain Generalization with Style Sharing (StyleDDG)

Input: $K, \mathcal{G} = (\mathcal{M}, \mathcal{E}), \{\alpha^{(k)}\}_{0 \leq k \leq K}$
Output: $\{\theta_i^{(K+1)}\}_{i \in \mathcal{M}}$

- 1 $k \leftarrow 0$, Initialize $\theta^{(0)}, \{\theta_i^{(0)} \leftarrow \theta^{(0)}\}_{i \in \mathcal{M}}$;
- 2 **while** $k \leq K$ **do**
- 3 **forall** $i \in \mathcal{M}$ **do**
- 4 sample mini-batch $(x_i^{(k)}, y_i^{(k)}) \in \mathcal{D}_i$;
- 5 calculate $\psi_i^{(k)} = \psi_{\theta_i^{(k)}}(x_i^{(k)})$ based on Eq. (15); share $\theta_i^{(k)}$
 and $\psi_i^{(k)}$ with neighbors \mathcal{N}_i ;
- 6 **forall** $i \in \mathcal{M}$ **do**
- 7 use the same mini-batch $(x_i^{(k)}, y_i^{(k)})$ from Line 4;
- 8 $g_i^{(k)} \leftarrow \nabla F_i(\theta_i^{(k)}, [\psi_j^{(k)}]_{j \in \mathcal{N}_i})$ (with respect to functions
 explained in Sec. 4.1.3);
- 9 $\text{aggr}_i^{(k)} \leftarrow 0$;
- 10 **forall** $j \in \mathcal{E}_i$ **do**
- 11 $p_{ij} \leftarrow 1/(1 + \max\{|\mathcal{N}_i|, |\mathcal{N}_j|\})$;
- 12 $\text{aggr}_i^{(k)} \leftarrow \text{aggr}_i^{(k)} + p_{ij}(\theta_j^{(k)} - \theta_i^{(k)})$;
- 13 **for** $i \in \mathcal{M}$ **do**
- 14 $\theta_i^{(k+1)} \leftarrow \theta_i^{(k)} + \text{aggr}_i^{(k)} - \alpha^{(k)} g_i^{(k)}$;
- 15 $k \leftarrow k + 1$;

4.2.2 *Local Loss.* We define the device-side local loss as

$$F_i(\theta, \Psi) = \sum_{\pi \in \mathcal{P}(L)} \left(\prod_{\ell \in \pi} p_\ell \right) \mathbb{E}_{(x, y) \sim \mathbb{P}_{D_i} \left[\mathcal{L}(\tilde{h}_{\theta, \{\psi_{j_\ell}, \mathcal{R}_\ell\}_{\ell \in \pi}}(x), y) \right],} \quad (21)$$

$\left\{ \begin{array}{l} j_\ell \in \mathcal{M} \setminus \{i\} \ell \in \pi \\ \mathcal{R}_\ell \sim \mathbb{P}_{\mathcal{R}} \ell \in \pi \end{array} \right.$

in which the expectation is taken over the set of random variables \mathcal{R}_ℓ defined as $\mathcal{R}_\ell = \{\epsilon_{\mu, \ell}, \epsilon_{\sigma, \ell}, \lambda_\ell, I_{s, \ell}, I_{e, \ell}, I_{m, \ell}\}$, and the entries are sampled from $\mathbb{P}_{\mathcal{R}} = \{\mathbb{P}_{\epsilon_\mu}, \mathbb{P}_{\epsilon_\sigma}, \mathbb{P}_\lambda, \mathfrak{S}_I, \mathfrak{S}_J, \mathfrak{S}_B\}$, respectively. \mathbb{P}_{D_i} denotes the probability distribution of source data in device $i \in \mathcal{M}$, and \mathfrak{S}_I is the set of all unique permutations of the set $I = \{0, \dots, 0, 1, \dots, 1\}$, which is a 0-1 vector of size B with the number of 0s and 1s each being equal to $B/2$. For a given layer ℓ , each device i utilizes the received styles of another device j in the training process, which is $\psi_{j_\ell} = [\bar{\mu}_{j_\ell} \quad \bar{\sigma}_{j_\ell} \quad \Sigma_{\mu, j_\ell}^2 \quad \Sigma_{\sigma, j_\ell}^2]^T$ as the j th element of Ψ in Eq. (21). What our method essentially does is applying a *style exploration* [31] strategy to the outputs of the model's layer ℓ with probability p_ℓ , so that the overall model is modified as

$$\tilde{h}_{\theta, \{\psi_{j_\ell}, \mathcal{R}_\ell\}_{\ell \in \pi}}(x) = \left(\tilde{h}_{\theta_L, \psi_{j_L}, \mathcal{R}_L} \circ \dots \circ \tilde{h}_{\theta_1, \psi_{j_1}, \mathcal{R}_1} \right)(x), \quad (22)$$

in which $\tilde{h}_{\theta_\ell, \psi_{j_\ell}, \mathcal{R}_\ell} = h_{\theta_\ell}$ if $\ell \notin \pi$. If $\ell \in \pi$, we define $x_s = [x_k]_{k \in \{1, \dots, B\}; (I_{s, \ell})_k = 1}$ as a subset of the mini-batch x based on the indices $I_{s, \ell}$ that we will shift to the styles of a neighboring device and $x_s^c = [x_k]_{k \in \{1, \dots, B\}; (I_{s, \ell})_k = 0}$ as the ones which will not be shifted. Then the StyleExplore update that occurs at that layer can be defined as

$$\tilde{h}_{\theta_\ell, \psi_{j_\ell}, \mathcal{R}_\ell}(x) = \text{StyleExplore}_{\substack{\lambda_{\ell, e}, \\ I_{m, \ell}, I_{e, \ell}}} \left(\text{StyleShift}_{\substack{\psi_{j_\ell}, \\ \epsilon_{\mu, \ell}, \epsilon_{\sigma, \ell}}}(h_{\theta_\ell}(x_s), h_{\theta_\ell}(x_s^c)) \right), \quad (23)$$

where we first apply the StyleShift function on a given mini-batch x to randomly shift half of the points to new styles received from a neighbor, and then the StyleExplore layer takes the outputs of the StyleShift function to randomly extrapolate half of those styles outwards for style exploration.

5 Convergence Analysis

In this section, we characterize the convergence behavior of our StyleDDG algorithm. Papers such as [17, 41, 43] prove that in decentralized optimization of general non-convex models, convergence to stationary points can be guaranteed if the local loss functions are smooth, i.e., their gradients are Lipschitz continuous. To this end, we will discuss the conditions under which the smoothness of local loss functions in StyleDDG given in Eq. (21) can be guaranteed as well. In other words, our goal is to prove that the upper bound $\|\nabla F_i(\theta, \Psi) - \nabla F_i(\theta', \Psi')\| \leq \beta_i \|\theta - \theta'\|$ can be established for each device in StyleDDG, where $\beta_i \in \mathbb{R}^+$ is the smoothness coefficient.

We also note that our main local loss function given in Eq. (21) essentially modifies the loss functions in a way that DG is achieved among the devices. We emphasize this to clarify what we mean by convergence in this context: whether the devices converge to the new optimal model with respect to the modified local loss functions.

5.1 Assumptions

We first make the following common assumption [17]:

ASSUMPTION 5.1. (*Multivariate smoothness*) *The local loss functions in StyleDDG given in Eq. (21) are smooth in their arguments, i.e.,*

$$\|\nabla F_i(\theta, \Psi) - \nabla F_i(\theta', \Psi')\| \leq \beta_{\theta, i} \|\theta - \theta'\| + \beta_{\Psi, i} \|\Psi - \Psi'\|, \quad (24)$$

in which $\beta_{\theta, i}, \beta_{\Psi, i} \in \mathbb{R}^+$ are positive scalars, $\theta, \theta' \in \mathbb{R}^n$ are any two model parameters and $\Psi, \Psi' \in \mathbb{R}^{|\mathcal{N}_i| \times L \times 4 \times C}$ are any two style vectors, for all $i \in \mathcal{M}$.

Assumption 5.1 is necessary to ensure the convergence of gradient-based methods, and it indicates that the local gradients do not change arbitrarily quickly [5]. Note that the conventional smoothness assumption made in [5, 17] is of the form $\|\nabla F_i(\theta) - \nabla F_i(\theta')\| \leq \beta_{\theta, i} \|\theta - \theta'\|$. These works do not modify their CNN models with any style-based statistics, and the local loss functions are parameterized by θ alone. Our Assumption 5.1 extends this to incorporate smoothness in terms of style vectors as well, i.e., the local loss functions do not change arbitrarily quickly with changes in the employed style statistics. See Appendix A for further discussion on the justification of this assumption.

REMARK 5.2. (*Multivariate smoothness justification*) *If we concatenate θ and Ψ to form the vector $\phi = [\theta^T, \Psi^T]^T$, then the left-hand side of Eq. (24) can also be bounded as*

$$\|\nabla F_i(\phi) - \nabla F_i(\phi')\| \leq \beta_{\phi, i} \|\phi - \phi'\|, \quad (25)$$

which is the standard smoothness assumption for a univariate function with $\beta_{\phi, i} \in \mathbb{R}^+$. Note that Eq. (25) is stricter than the multivariate smoothness assumption we use in Eq. (24) since we can obtain the former from the latter using triangle inequality.

Additionally, we presume three constraints on the CNN outputs:

ASSUMPTION 5.3. For each device $i \in \mathcal{M}$ and layer $\ell \in \{1, \dots, L\}$ of the CNN θ , the following holds for the outputs $h_{\theta_\ell}(x_i)$ given an input x_i for device i :

(a) (Lipschitz continuity of layer outputs) We have

$$\|h_{\theta_\ell}(x_i)_{b,c,h,w} - h_{\theta'_\ell}(x_i)_{b,c,h,w}\| \leq D_{i,\ell} \|\theta - \theta'\|, \quad (26)$$

where $\theta, \theta' \in \mathbb{R}^n$ are two arbitrary model parameters and $D_{i,\ell} \in \mathbb{R}^+$ is a positive scalar. Also, we define $D_i = \max_\ell \{D_{i,\ell}\}$ and $D = \max_i \{D_i\}$.

(b) (Bounded layer outputs) We further assume that for all $\theta \in \mathbb{R}^n$, there exists $U_{i,\ell} \in \mathbb{R}^+$ such that

$$\max_{\theta_\ell, x_i} \{\|h_{\theta_\ell}(x_i)_{b,c,h,w}\|\} \leq U_{i,\ell} < \infty. \quad (27)$$

Also, we define $U_i = \max_\ell \{U_{i,\ell}\}$ and $U = \max_i \{U_i\}$.

(c) (Positive standard deviation of layer outputs) Finally, for all $\theta \in \mathbb{R}^n$, we assume that there exists $\gamma_{i,\ell} \in \mathbb{R}^+$ such that

$$\|\sigma(h_{\theta_\ell}(x_i))_{b,c}\| \geq \min_{\theta_\ell, x_i} \{\|\sigma(h_{\theta_\ell}(x_i))_{b,c}\|\} \geq \gamma_{i,\ell} > 0, \quad (28)$$

where $\sigma(\cdot)_{b,c}$ is as defined in Eq. (2). Also, we define $\gamma_i = \min_\ell \{\gamma_{i,\ell}\}$ and $\gamma = \min_i \{\gamma_i\}$.

Assumption 5.3-(a) indicates that changes in the model parameters θ does not lead to arbitrary large changes in the outputs of any layer. This is a safe assumption to make as the operations in CNNs (e.g., convolutional blocks, pooling layers and activation functions) behave this way. Assumption 5.3-(b) depends on the particular activation functions being used at a specific layer of the CNN. For example, this assumption always holds for sigmoid, tanh and other bounded activation functions. For ReLU and other unbounded activations, although the function is not bounded mathematically, for the purpose of our analysis we only need this assumption to hold during the training phase of our method. Assumption 5.3-(c) indicates that for an instance of the batch b and a particular channel c of the ℓ th layer of the CNN, the standard deviation of $H_\ell \times W_\ell$ dimensional output can be lower bounded for all possible inputs in the dataset and all possible models θ . In a nutshell, this assumption helps us guarantee that the outputs of the CNN layers will not be identical for different inputs/models.

5.2 Main Results

In this section, we first provide a useful Lemma which follows Assumption 5.3-(b) on the boundedness of μ and σ style statistics. Then, we will use this Lemma to prove a key result in Proposition 5.5 and Lemma 5.6, which provide guarantees for the smoothness of local loss functions in StyleDDG. Finally, in Theorem 5.7, we will use these results to show the convergence of StyleDDG for general non-convex loss functions.

LEMMA 5.4. (Bounded μ and σ style statistics) Let Assumption 5.3-(b) hold. Then for all devices $i \in \mathcal{M}$ and all layers/blocks $\ell \in \{1, \dots, L\}$ of the CNN θ it holds that

- (a) $\|\mu(h_{\theta_\ell}(x_i))_{b,c}\| \leq U_{i,\ell}$,
- (b) $\|\sigma(h_{\theta_\ell}(x_i))_{b,c}\| \leq \sqrt{2}U_{i,\ell}$,
- (c) $\|\bar{\mu}_{\theta_\ell}(x_i)_c\| \leq U_{i,\ell}$.
- (d) $\|\bar{\sigma}_{\theta_\ell}(x_i)_c\| \leq \sqrt{2}U_{i,\ell}$,

where $U_{i,\ell}$ is provided in Assumption 5.3.

See Appendix B for the proof.

Note that Assumption 5.3-(c) together with Lemma 5.4-(b) establish the bounds $\gamma_{i,\ell} \leq \|\sigma(h_{\theta_\ell}(x_i))_{b,c}\| \leq U_{i,\ell}$.

Equipped with Lemma 5.4, we move on to presenting the next key result which establishes the Lipschitz continuity of all style statistics used in StyleDDG. Our high-level goal in showing this result is to ultimately prove that the second term in our smoothness assumption given in Eq. (24), i.e., $\|\Psi - \Psi'\|$, can also be bounded by $\|\theta - \theta'\|$.

PROPOSITION 5.5. (Lipschitz continuity of style statistics) Let Assumption 5.3 hold. Then the style statistics from Eq. (15) are Lipschitz continuous at each layer/block $\ell = \{1, \dots, L\}$ of the CNN θ for all devices $i \in \mathcal{M}$, and for all channels $c \in \{1, \dots, C\}$. Specifically:

- (a) $\|\bar{\mu}_{\theta_\ell}(x_i)_c - \bar{\mu}_{\theta'_\ell}(x_i)_c\| \leq D_{i,\ell} \|\theta - \theta'\|$,
- (b) $\|\bar{\sigma}_{\theta_\ell}(x_i)_c - \bar{\sigma}_{\theta'_\ell}(x_i)_c\| \leq \frac{4U_{i,\ell}D_{i,\ell}}{\gamma_{i,\ell}} \|\theta - \theta'\|$,
- (c) $\|\Sigma_{\mu,\theta_\ell}^2(x_i)_c - \Sigma_{\mu,\theta'_\ell}^2(x_i)_c\| \leq 4U_{i,\ell}D_{i,\ell} \|\theta - \theta'\|$,
- (d) $\|\Sigma_{\sigma,\theta_\ell}^2(x_i)_c - \Sigma_{\sigma,\theta'_\ell}^2(x_i)_c\| \leq 4U_{i,\ell}D_{i,\ell} \left(1 + \frac{2\sqrt{2}U_{i,\ell}}{\gamma_{i,\ell}}\right) \|\theta - \theta'\|$.

See Appendix C for the proof.

Proposition 5.5 shows that if the style statistics given in Eq. (15) are calculated via the model θ on any data batch X , the resulting statistics will be Lipschitz with respect to θ . With this result in hand, we can now prove the smoothness of local and global loss functions given in Eqs. (21) and (20), respectively.

LEMMA 5.6. (Univariate smoothness) Let Assumptions 5.1 and 5.3 hold. Then for any $\theta, \theta' \in \mathbb{R}^n$, it holds that

- (a) (Smoothness of local loss functions) For any given combined batch X for all devices, the local loss function of each device $i \in \mathcal{M}$ is smooth, i.e.,

$$\|\nabla F_i(\theta, \Psi_{\theta,i}(X)) - \nabla F_i(\theta', \Psi_{\theta',i}(X))\| \leq \beta_i \|\theta - \theta'\|, \quad (29)$$

with $\beta_i = \beta_{\theta,i} + mL \left(1 + 4U \left(1/\gamma + 2 + (2\sqrt{2}U)/\gamma\right)\right) D\beta_{\Psi,i}$, where $\beta_{\theta,i}$ and $\beta_{\Psi,i}$ are provided in Assumption 5.1, m is the total number of devices, L is the number of layers which StyleDDG is applied to, and U , D and γ are the bounds of Assumption 5.3.

- (b) (Smoothness of the global loss function) The global loss function is smooth, i.e.,

$$\|\nabla F(\theta) - \nabla F(\theta')\| \leq \beta \|\theta - \theta'\|, \quad (30)$$

with $\beta = (1/m) \sum_{i=1}^m \beta_i$.

See Appendix D for the proof.

In Lemma 5.6-(a), note that a smaller value of $U = \max_{i,\ell} U_{i,\ell}$ and $D = \max_{i,\ell} D_{i,\ell}$, and a larger value of $\gamma = \min_{i,\ell} \gamma_{i,\ell}$ results in a smaller smoothness parameter β . This corresponds to a faster convergence during training. See Appendix A for further discussions.

THEOREM 5.7. Let Assumptions 5.1 and 5.3 hold, and a constant learning rate $\alpha^{(k)} = \alpha^{(0)}/\sqrt{K+1}$ be employed where K is the maximum number of iterations that StyleDDG will run. Then, for general non-convex loss model, we have

$$\frac{\sum_{k=0}^K \|\nabla F(\bar{\theta}^{(k)})\|^2}{K+1} \leq \frac{F(\bar{\theta}^{(0)}) - F^* + \beta/(2m)}{O(\sqrt{K+1})} + \frac{1+\rho}{(1-\rho)^2} \frac{\beta^2}{O(K+1)}, \quad (31)$$

| METHOD | ACCURACY FOR TARGET DOMAIN | | | | |
|------------------|----------------------------|-------------------|-------------------|-------------------|-------------|
| | ART | CARTOON | PHOTO | SKETCH | AVG |
| FEDBN | 53.6 ± 0.9 | 48.9 ± 1.6 | 74.0 ± 1.9 | 53.4 ± 5.5 | 57.5 |
| FEDBN + MixStyle | 59.7 ± 1.5 | 55.5 ± 1.7 | 78.2 ± 1.0 | 55.7 ± 3.0 | 62.3 |
| FEDBN + DSU | 59.5 ± 1.0 | 55.9 ± 2.5 | 79.0 ± 1.4 | 59.7 ± 3.9 | 63.5 |
| DSGD | 67.7 ± 2.3 | 67.8 ± 1.1 | 91.1 ± 0.6 | 53.0 ± 9.9 | 69.9 |
| DSGD + MixStyle | 74.7 ± 1.0 | 71.1 ± 2.1 | 91.1 ± 0.5 | 58.9 ± 4.1 | 73.9 |
| DSGD + DSU | 76.6 ± 0.7 | 71.8 ± 1.0 | 91.7 ± 0.2 | 63.6 ± 3.0 | 75.9 |
| StyleDDG | 77.7 ± 0.4 | 73.0 ± 0.4 | 94.2 ± 0.3 | 66.2 ± 0.6 | 77.8 |

Table 1: Results on the PACS dataset, for a network of $m = 3$ devices all connected to each other.

| METHOD | ACCURACY FOR TARGET DOMAIN | | | | |
|------------------|----------------------------|-------------------|-------------------|-------------------|-------------|
| | ART | CARTOON | PHOTO | SKETCH | AVG |
| FEDBN | 40.2 ± 0.9 | 35.5 ± 0.3 | 52.7 ± 1.4 | 34.0 ± 0.7 | 40.6 |
| FEDBN + MixStyle | 42.2 ± 1.0 | 39.1 ± 0.3 | 53.6 ± 1.4 | 38.6 ± 0.2 | 43.4 |
| FEDBN + DSU | 42.6 ± 0.8 | 40.8 ± 0.8 | 56.8 ± 2.4 | 39.3 ± 0.6 | 44.9 |
| DSGD | 58.8 ± 1.1 | 52.5 ± 2.1 | 78.0 ± 2.0 | 36.7 ± 5.2 | 56.5 |
| DSGD + MixStyle | 60.8 ± 1.4 | 55.6 ± 1.9 | 73.3 ± 0.9 | 39.9 ± 4.9 | 57.4 |
| DSGD + DSU | 56.8 ± 1.2 | 54.1 ± 1.7 | 78.2 ± 3.4 | 35.5 ± 4.8 | 56.1 |
| StyleDDG | 60.6 ± 1.6 | 56.3 ± 2.0 | 81.5 ± 4.0 | 42.3 ± 4.5 | 60.2 |

Table 2: Results on the PACS dataset, for a network of $m = 9$ devices over a random geometric graph with radius 0.8.

in which $F^* = \min_{\theta \in \mathbb{R}^n} \{F(\theta)\}$, m denotes the number of devices, $\bar{\theta}^{(k)} = (1/m) \sum_{i=1}^m \theta_i^{(k)}$ is the average model among all devices at iteration k , ρ captures the spectral radius of the network graph \mathcal{G} and β is the smoothness parameter given by Lemma 5.6-(b).

See Appendix E for the proof.

Theorem 5.7 shows that StyleDDG reaches a stationary point for general non-convex models at a rate of $\mathcal{O}(1/\sqrt{K})$. To be specific, after running StyleDDG for K iterations with a learning rate proportional to $1/\sqrt{K+1}$, the running average $(\frac{1}{K+1} \sum_{k=0}^K (\cdot))$ of global gradient norm expectations $(\mathbb{E}[\|\nabla F(\cdot)\|])$ evaluated at the average model $\bar{\theta}^{(k)}$, is proportional to $1/\sqrt{K+1}$. Therefore, this bound becomes arbitrarily small as the training progresses, i.e., by increasing K . Further, in Theorem 5.7, problem-related parameters of Assumptions 5.1 and 5.3, i.e., multivariate smoothness parameters $\beta_{\theta,i}$ and $\beta_{\Psi,i}$, Lipschitz constant $D_{i,\ell}$, upper bound $U_{i,\ell}$ and lower bound $\gamma_{i,\ell}$, are all captured in the univariate smoothness parameter β derived in Lemma 5.6. We see in Eq. (31) that a lower smoothness value β and a better-connected graph, i.e., smaller spectral radius ρ , results in a smaller upper bound in Eq. (31). Consequently, in such cases, convergence is achieved in a lower number of total iterations K .

6 Numerical Experiments

6.1 Setup

Datasets and Model. Our experiments are based on two widely-used benchmark datasets for DG: (i) PACS [19] which consists of 4 domains (art painting (A), cartoon (C), photo (P), and sketch (S)) and contains 7 classes of images (dog, elephant, giraffe, guitar, horse, house, and person); (ii) VLCS [34] with 4 domains (Caltech101, LabelMe, PASCAL VOC2007 and SUN09) and 5 categories of images (bird, car, chair, dog, and person). For both datasets, we use 3 domains as the source domains and reserve the remaining one as the

| METHOD | ACCURACY FOR TARGET DOMAIN | | | | |
|------------------|----------------------------|-------------------|-------------------|-------------------|-------------|
| | CALTECH | LABELME | PASCAL | SUN | AVG |
| FEDBN | 95.5 ± 0.8 | 56.6 ± 0.5 | 65.1 ± 0.7 | 66.1 ± 0.6 | 70.8 |
| FEDBN + MixStyle | 96.7 ± 0.5 | 57.2 ± 0.5 | 65.8 ± 0.4 | 66.9 ± 0.7 | 71.6 |
| FEDBN + DSU | 97.4 ± 0.2 | 56.5 ± 0.3 | 66.4 ± 0.3 | 67.1 ± 0.4 | 71.9 |
| DSGD | 96.3 ± 0.8 | 56.0 ± 0.5 | 67.9 ± 0.6 | 68.5 ± 1.0 | 72.2 |
| DSGD + MixStyle | 98.0 ± 0.6 | 56.9 ± 0.7 | 67.7 ± 1.8 | 70.1 ± 1.4 | 73.2 |
| DSGD + DSU | 98.4 ± 0.3 | 56.1 ± 0.3 | 68.6 ± 0.6 | 69.9 ± 1.4 | 73.2 |
| StyleDDG | 98.6 ± 0.8 | 58.1 ± 1.2 | 69.4 ± 0.1 | 69.4 ± 1.4 | 73.9 |

Table 3: Results on the VLCS dataset, for a network of $m = 3$ devices all connected to each other.

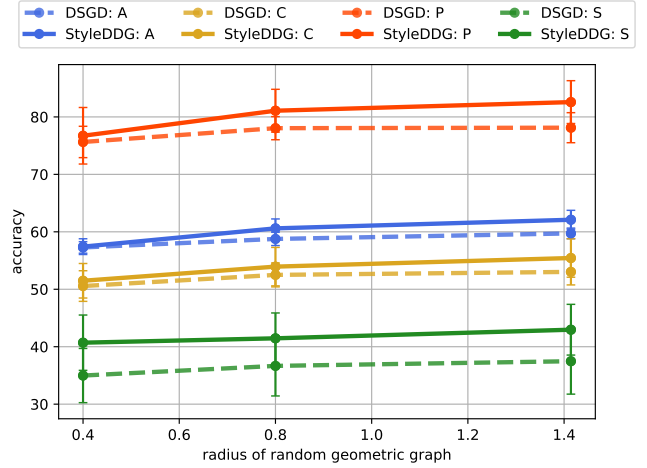


Figure 4: Results on the PACS dataset for different target domains, for a network of $m = 9$ clients over a random geometric graph with varying radius.

target domain (for evaluating the test performance). We conduct our experiments using the standard ResNet18 model [11].

Baselines. Since our work is the first to propose a fully decentralized DG algorithm, we select some centralized and federated DG algorithms and implement a decentralized realization of them for comparison. Specifically, we compare StyleDDG against DSGD [17], FedBN [23], MixStyle [49] and DSU [22]. For the well-known style-based centralized DG methods, MixStyle and DSU, we incorporate these algorithms into the local update process at each client.

Setting. Our experiments are done under two sets of networks (i) a network of $m = 3$ edge devices and (ii) a network with $m = 9$ edge devices connected together over a random geometric graph [32]. The choice of 3-9 edge devices aligns with the conventions of experiments found in existing FDG literature [23, 29, 45], to provide fair comparisons with the baselines. Our implementation of StyleDDG is based on the dassl library developed in [47, 48]. We adopt a constant learning rate $\alpha = 0.001$ with a cosine scheduler, and use the batch size of 64. We distribute the data among the edge devices in a domain-heterogeneous way, i.e., each device receives samples only from a single domain. We measure the test accuracy of each algorithm achieved after 50 epochs of training. We conduct the experiments based on a cluster of four NVIDIA A100 GPUs with 40GB memory. We run the experiments five times in each setup, and present the mean and 1-sigma standard deviation.

6.2 Results and Discussion

PACS. Table 1 shows the result with PACS dataset with $m = 3$ clients. We make the following observations. First, existing style-based centralized DG methods, i.e., MixStyle and DSU, enhance the performance of both FedBN and DSGD by exposing models to a diversity of styles. However, applying these approaches does not allow the model to sufficiently explore diverse styles, as each device has access to only a limited set of styles or domains. We observe that StyleDDG addresses this limitation through style sharing and exploration in decentralized settings, resulting in a significant improvement in generalization capability.

Table 2 extends our results to a network of $m = 9$ devices connected via a random geometric graph with a radius of 0.8. We see that the performance gain of StyleDDG over the baselines becomes more pronounced, highlighting its advantage in larger networks with less connectivity among devices.

VLCS. In Table 3, we also evaluate performance on another dataset, VLCS. Although the gains are smaller than those observed on PACS – due to the relatively smaller style gap between domains in VLCS [31] – StyleDDG still outperforms on all but one domain.

Graph connectivity. In Fig. 4, we vary radius of the random geometric graph in a network of $m = 9$ devices and compare the performance of StyleDDG with DSDG for different connectivity levels of the network. We observe that our methodology maintains its superiority across different connectivity levels. Furthermore, the advantage of our method increases with higher graph connectivity, showing that it can better utilize the underlying device network to achieve DG. In other words, the strength of style sharing in our method becomes more significant if each device is connected to more neighbors, as it can be exposed to a larger set of styles beyond its own.

7 Conclusion

We proposed StyleDDG, one of the first decentralized federated domain generalization algorithms. StyleDDG enables edge devices in a decentralized network to train domain-invariant models. We achieved this by forming consensus-based model aggregation and style sharing, and developing a style exploration strategy to expose each device to the new style domains received from their neighbors. Furthermore, we provided a novel analytical foundation of well-known domain generalization methods and extended it to our methodology, enabling us to conduct convergence analysis on StyleDDG, the first such analysis among all style-based domain generalization algorithms. Our experiments demonstrated the effectiveness of StyleDDG compared to other domain generalization baselines in terms of model accuracy on unseen target domains.

References

- [1] Jimmy Lei Ba, Jamie Ryan Kiros, and Geoffrey E Hinton. 2016. Layer normalization. *arXiv preprint arXiv:1607.06450* (2016).
- [2] Ruqi Bai, Saurabh Bagchi, and David I Inouye. 2024. Benchmarking Algorithms for Federated Domain Generalization. In *ICLR*.
- [3] Yogesh Balaji, Swami Sankaranarayanan, and Rama Chellappa. 2018. Metareg: Towards domain generalization using meta-regularization. *NeurIPS* 31 (2018).
- [4] Shai Ben-David, John Blitzer, Koby Crammer, Alex Kulesza, Fernando Pereira, and Jennifer Wortman Vaughan. 2010. A theory of learning from different domains. *Machine learning* 79 (2010), 151–175.
- [5] Léon Bottou, Frank E Curtis, and Jorge Nocedal. 2018. Optimization methods for large-scale machine learning. *SIAM review* 60, 2 (2018), 223–311.
- [6] Christopher G Brinton, Mung Chiang, Kwang Taik Kim, David J Love, Michael Beesley, Morris Repeta, John Roesse, Per Beming, Erik Ekudden, Clara Li, et al. 2025. Key focus areas and enabling technologies for 6G. *IEEE Communications Magazine* 63, 3 (2025), 84–91.
- [7] Fabio M Carlucci, Antonio D’Innocente, Silvia Bucci, Barbara Caputo, and Tatiana Tommasi. 2019. Domain generalization by solving jigsaw puzzles. In *IEEE CVPR*. 2229–2238.
- [8] Evan Chen, Shiqiang Wang, and Christopher G Brinton. 2024. Taming subnet-drift in D2D-enabled fog learning: A hierarchical gradient tracking approach. In *IEEE INFOCOM*. 2438–2447.
- [9] Junming Chen, Meirui Jiang, Qi Dou, and Qifeng Chen. 2023. Federated domain generalization for image recognition via cross-client style transfer. In *IEEE/CVF WACV*. 361–370.
- [10] Muhammad Ghifary, W Bastiaan Kleijn, Mengjie Zhang, and David Balduzzi. 2015. Domain generalization for object recognition with multi-task autoencoders. In *ICCV*. 2551–2559.
- [11] Kaiming He, Xiangyu Zhang, Shaoqing Ren, and Jian Sun. 2016. Deep residual learning for image recognition. In *IEEE CVPR*. 770–778.
- [12] Seyyedali Hosseinalipour, Christopher G Brinton, Vaneet Aggarwal, Huaiyi Dai, and Mung Chiang. 2020. From federated to fog learning: Distributed machine learning over heterogeneous wireless networks. *IEEE Communications Magazine* 58, 12 (2020), 41–47.
- [13] Xun Huang and Serge Belongie. 2017. Arbitrary style transfer in real-time with adaptive instance normalization. In *ICCV*. 1501–1510.
- [14] Yudi Huang, Tingyang Sun, and Ting He. 2024. Overlay-based Decentralized Federated Learning in Bandwidth-limited Networks. In *ACM MobiHoc*. 121–130.
- [15] Zeyi Huang, Haohan Wang, Eric P King, and Dong Huang. 2020. Self-challenging improves cross-domain generalization. In *ECCV*. Springer, 124–140.
- [16] Sergey Ioffe and Christian Szegedy. 2015. Batch normalization: Accelerating deep network training by reducing internal covariate shift. In *ICML*. pmlr, 448–456.
- [17] Anastasia Koloskova, Nicolas Loizou, Sadra Boreiri, Martin Jaggi, and Sebastian Stich. 2020. A unified theory of decentralized sgd with changing topology and local updates. In *ICML*. PMLR, 5381–5393.
- [18] Da Li, Yongxin Yang, Yi-Zhe Song, and Timothy Hospedales. 2018. Learning to generalize: Meta-learning for domain generalization. In *AAAI*, Vol. 32.
- [19] Da Li, Yongxin Yang, Yi-Zhe Song, and Timothy M Hospedales. 2017. Deeper, broader and artier domain generalization. In *ICCV*. 5542–5550.
- [20] Haoliang Li, Simo Jialin Pan, Shiqi Wang, and Alex C Kot. 2018. Domain generalization with adversarial feature learning. In *IEEE CVPR*. 5400–5409.
- [21] Tian Li, Anit Kumar Sahu, Ameet Talwalkar, and Virginia Smith. 2020. Federated learning: Challenges, methods, and future directions. *IEEE signal processing magazine* 37, 3 (2020), 50–60.
- [22] Xiaotong Li, Yongxing Dai, Yixiao Ge, Jun Liu, Ying Shan, and Ling-Yu Duan. 2022. Uncertainty modeling for out-of-distribution generalization. *ICLR* (2022).
- [23] Xiaoxiao Li, Meirui JIANG, Xiaofei Zhang, Michael Kamp, and Qi Dou. 2021. FedBN: Federated Learning on Non-IID Features via Local Batch Normalization. In *ICLR*.
- [24] Ying Li, Xingwei Wang, Rongfei Zeng, Praveen Kumar Donta, Ilir Murturi, Min Huang, and Schahram Dustdar. 2023. Federated domain generalization: A survey. *arXiv preprint arXiv:2306.01334* (2023).
- [25] Wei Liu, Li Chen, and Weidong Wang. 2022. General decentralized federated learning for communication-computation tradeoff. In *IEEE INFOCOM WKSHPs*. 1–6.
- [26] Brendan McMahan, Eider Moore, Daniel Ramage, Seth Hampson, and Blaise Aguerre y Arcas. 2017. Communication-efficient learning of deep networks from decentralized data. In *AISTATS*. PMLR, 1273–1282.
- [27] Angelia Nedić, Alex Olshevsky, and Michael G Rabbat. 2018. Network topology and communication-computation tradeoffs in decentralized optimization. *Proc. IEEE* 106, 5 (2018), 953–976.
- [28] Angelia Nedic and Asuman Ozdaglar. 2009. Distributed subgradient methods for multi-agent optimization. *IEEE Trans. Automat. Control* 54, 1 (2009), 48–61.
- [29] A Tuan Nguyen, Philip Torr, and Ser Nam Lim. 2022. Fedrs: A simple and effective domain generalization method for federated learning. In *NeurIPS*, Vol. 35. 38831–38843.
- [30] Rohit Parasnin, Seyyedali Hosseinalipour, Yun-Wei Chu, Mung Chiang, and Christopher G Brinton. 2023. Connectivity-aware semi-decentralized federated learning over time-varying D2D networks. In *ACM MobiHoc*. 31–40.
- [31] Jungwuk Park, Dong-Jun Han, Jinho Kim, Shiqiang Wang, Christopher Brinton, and Jaekyun Moon. 2024. StableFDG: style and attention based learning for federated domain generalization. *NeurIPS* 36 (2024).
- [32] Mathew Penrose. 2003. *Random geometric graphs*. Vol. 5. OUP Oxford.
- [33] Shibani Santurkar, Dimitris Tsipras, Andrew Ilyas, and Aleksander Madry. 2018. How does batch normalization help optimization? *NeurIPS* 31 (2018).
- [34] Antonio Torralba and Alexei A Efros. 2011. Unbiased look at dataset bias. In *IEEE CVPR*. IEEE, 1521–1528.
- [35] Dmitry Ulyanov, Andrea Vedaldi, and Victor Lempitsky. 2016. Instance normalization: The missing ingredient for fast stylization. *arXiv preprint arXiv:1607.08022* (2016).

- [36] Jindong Wang, Cuiling Lan, Chang Liu, Yidong Ouyang, Tao Qin, Wang Lu, Yiqiang Chen, Wenjun Zeng, and S Yu Philip. 2022. Generalizing to unseen domains: A survey on domain generalization. *IEEE transactions on knowledge and data engineering* 35, 8 (2022), 8052–8072.
- [37] Su Wang, Seyyedali Hosseinalipour, and Christopher G Brinton. 2024. Multi-source to multi-target decentralized federated domain adaptation. *IEEE Transactions on Cognitive Communications and Networking* 10, 3 (2024), 1011–1025.
- [38] Guile Wu and Shaogang Gong. 2021. Collaborative optimization and aggregation for decentralized domain generalization and adaptation. In *ICCV*. 6484–6493.
- [39] Yuxin Wu and Kaiming He. 2018. Group normalization. In *ECCV*. 3–19.
- [40] Lin Xiao and Stephen Boyd. 2004. Fast linear iterations for distributed averaging. *Systems & Control Letters* 53, 1 (2004), 65–78.
- [41] Ran Xin, Usman A Khan, and Soumya Kar. 2021. An improved convergence analysis for decentralized online stochastic non-convex optimization. *IEEE Transactions on Signal Processing* 69 (2021), 1842–1858.
- [42] Jingjing Xu, Xu Sun, Zhiyuan Zhang, Guangxiang Zhao, and Junyang Lin. 2019. Understanding and improving layer normalization. *NeurIPS* 32 (2019).
- [43] Shahryar Zehtabi, Dong-Jun Han, Rohit Parasnisi, Seyyedali Hosseinalipour, and Christopher G Brinton. 2025. Decentralized Sporadic Federated Learning: A Unified Methodology with Generalized Convergence Guarantees. *ICLR* (2025).
- [44] Jie Zhang, Li Chen, Xiaohui Chen, and Guo Wei. 2023. A novel hierarchically decentralized federated learning framework in 6G wireless networks. In *INFOCOM WKSHPS*. IEEE, 1–6.
- [45] Liling Zhang, Xinyu Lei, Yichun Shi, Hongyu Huang, and Chao Chen. 2021. Federated learning with domain generalization. *arXiv preprint arXiv:2111.10487* (2021).
- [46] Xin Zhang, Minghong Fang, Zhuqing Liu, Haibo Yang, Jia Liu, and Zhengyuan Zhu. 2022. Net-fleet: Achieving linear convergence speedup for fully decentralized federated learning with heterogeneous data. In *ACM MobiHoc*. 71–80.
- [47] Kaiyang Zhou, Ziwei Liu, Yu Qiao, Tao Xiang, and Chen Change Loy. 2022. Domain generalization: A survey. *IEEE Transactions on Pattern Analysis and Machine Intelligence* 45, 4 (2022), 4396–4415.
- [48] Kaiyang Zhou, Yongxin Yang, Yu Qiao, and Tao Xiang. 2021. Domain adaptive ensemble learning. *IEEE Transactions on Image Processing* 30 (2021), 8008–8018.
- [49] Kaiyang Zhou, Yongxin Yang, Yu Qiao, and Tao Xiang. 2021. Domain generalization with mixstyle. *ICLR* (2021).

A Smoothness Assumption

In Assumption 5.1, we assumed that the local loss functions $F_i(\theta, \Psi)$ for all devices $i \in \mathcal{M}$ have Lipschitz gradients in terms of both its arguments θ and Ψ , i.e., $\|\nabla F_i(\theta, \Psi) - \nabla F_i(\theta', \Psi')\| \leq \beta_{\theta,i} \|\theta - \theta'\| + \beta_{\Psi,i} \|\Psi - \Psi'\|$. While having the term $\beta_{\theta,i} \|\theta - \theta'\|$ in the upper bound is quite standard in the literature [5], we will justify the $\beta_{\Psi,i} \|\Psi - \Psi'\|$ term in the upper bound in this Appendix.

In the core of all style-based algorithms, we ultimately apply the AdaIN operation [13] given in Eq. (1). This function is first applying instance normalization to the outputs of a layer by calculating $(x - \mu(x))/\sigma(x)$, and then scales and shifts it adaptively to another style characterized by μ_t and σ_t . If μ_t and σ_t are constant-value vectors, or are trainable parameters, then AdaIN reduces down to Instance Normalization [35], in which a normalization is applied to each instance of the batch individually. Instance Normalization itself can be considered as a special case of Group Normalization [39] where each channel group consists of only one channel, and the normalization is applied to each channel group separately. Note that if put all the channels into one group, we get Layer Normalization [1] where the normalization is applied to each instance of the batch across all channels together. Finally, note that most well-known Batch Normalization [16] applies the normalization across each individual channel separately, but does so by considering all the instances in the batch together.

Consequently, InstanceNorm can be obtained by setting the batch size to one in BatchNorm, or processing each channel one at a time in LayerNorm. Motivated by this observation, we will use existing results on the smoothness of BatchNorm and LayerNorm to justify the smoothness of InstanceNorm. Note, however, that a

standalone analysis of InstanceNorm and AdaIN is necessary for rigorous characterization of the smoothness of AdaIN, but this is outside of the scope of our paper as our main goal is to analyze the convergence behavior of a decentralized optimization algorithm aiming to achieve domain generalization.

[33] analyzes the effect of Batch Normalization on the smoothness of the loss function in centralized training. They conclude that adding BatchNorm layers to a CNN model results in the optimization landscape to become smoother. [42] make a similar analysis for Layer Normalization, in which it is shown that adding LayerNorm layers result in smoother gradients. Our Assumption 5.1 is motivated by these analytical results.

We should note that the above-mentioned analytical results [33, 42] show an improvement in smoothness, i.e., lower $\beta_{\theta,i}$ in Eq. (24). However, this result holds when the scaling and shifting parameters of BatchNorm and LayerNorm (of similar nature to μ_t and σ_t of AdaIN given in Eq. (1)) are trainable. In contrast for AdaIN, μ_t and σ_t are calculated based on the style statistics of a set of data points, and is thus not trainable. It is important to note that in this case, although a better smoothness of local loss functions is not guaranteed, but the smoothness property is still preserved [33].

B Proof of Lemma 5.4

PROOF. (a) Using the definition of $\mu(\cdot)_{b,c}$ from Eq. (2), we have

$$\begin{aligned} \|\mu(h_{\theta_t}(x_i))_{b,c}\| &= \left\| \frac{1}{HW} \sum_{h=1}^H \sum_{w=1}^W h_{\theta_t}(x_i)_{b,c,h,w} \right\| \\ &\leq \frac{1}{HW} \sum_{h=1}^H \sum_{w=1}^W \|h_{\theta_t}(x_i)_{b,c,h,w}\| \leq \frac{1}{HW} \sum_{h=1}^H \sum_{w=1}^W U_{i,\ell} = U_{i,\ell}, \end{aligned} \quad (32)$$

in which we used the triangle inequality. \square

PROOF. (b) We first find an upper bound for $\|\sigma^2(h_{\theta_t}(x_i))_{b,c}\|$, and then take the square root of those to conclude the proof. Using the definition of $\sigma^2(\cdot)_{b,c}$ from Eq. (2), we first rewrite its definition as

$$\begin{aligned} \sigma^2(h_{\theta_t}(x_i))_{b,c} &= \frac{1}{HW} \sum_{h=1}^H \sum_{w=1}^W (h_{\theta_t}(x_i)_{b,c,h,w} - \mu(h_{\theta_t}(x_i))_{b,c})^2 \\ &= \frac{1}{HW} \sum_{h=1}^H \sum_{w=1}^W h_{\theta_t}(x_i)_{b,c,h,w}^2 - \mu(h_{\theta_t}(x_i))_{b,c}^2. \end{aligned} \quad (33)$$

Using this definition, we can write the following

$$\begin{aligned} \|\sigma^2(h_{\theta_t}(x_i))_{b,c}\| &= \left\| \frac{1}{HW} \sum_{h=1}^H \sum_{w=1}^W h_{\theta_t}(x_i)_{b,c,h,w}^2 - \mu(h_{\theta_t}(x_i))_{b,c}^2 \right\| \\ &\leq \frac{1}{HW} \sum_{h=1}^H \sum_{w=1}^W \|h_{\theta_t}(x_i)_{b,c,h,w}^2\| + \|\mu(h_{\theta_t}(x_i))_{b,c}^2\| \\ &\leq \frac{1}{HW} \sum_{h=1}^H \sum_{w=1}^W U_{i,\ell}^2 + U_{i,\ell}^2 = 2U_{i,\ell}^2, \end{aligned} \quad (34)$$

in which we used the triangle inequality, and then invoked the results of Assumption 5.3-(b) and Lemma 5.4-(a). \square

PROOF. (c) Using the definition of $\bar{\mu}_{\theta,\ell}(x_i)_c$ from Eq. (15), we have

$$\begin{aligned} \|\bar{\mu}_{\theta,\ell}(x_i)_c\| &= \left\| \frac{1}{B} \sum_{b=1}^B \mu(h_{\theta_\ell}(x_i))_{b,c} \right\| \\ &\leq \frac{1}{B} \sum_{b=1}^B \|\mu(h_{\theta_\ell}(x_i))_{b,c}\| \leq \frac{1}{B} \sum_{b=1}^B U_{i,\ell} = U_{i,\ell}, \end{aligned} \quad (35)$$

in which we used the triangle inequality and then invoked the result of Lemma 5.4-(a). \square

PROOF. (d) Using the definition of $\bar{\sigma}_{\theta,\ell}(x_i)_c$ from Eq. (15), we have

$$\begin{aligned} \|\bar{\sigma}_{\theta,\ell}(x_i)_c\| &= \left\| \frac{1}{B} \sum_{b=1}^B \sigma(h_{\theta_\ell}(x_i))_{b,c} \right\| \leq \frac{1}{B} \sum_{b=1}^B \|\sigma(h_{\theta_\ell}(x_i))_{b,c}\| \\ &\leq \frac{1}{B} \sum_{b=1}^B \sqrt{2}U_{i,\ell} = \sqrt{2}U_{i,\ell}, \end{aligned} \quad (36)$$

in which we used the triangle inequality and then invoked the result of Lemma 5.4-(b). \square

C Proof of Proposition 5.5

PROOF. (a) Using the definition $\bar{\mu}_{\theta,\ell}(x_i)_c = \frac{1}{B} \sum_{b=1}^B \mu(h_{\theta_\ell}(x_i))_{b,c}$ given in Eq. (15), we have that

$$\begin{aligned} &\|\bar{\mu}_{\theta,\ell}(x_i)_c - \bar{\mu}_{\theta',\ell}(x_i)_c\| \\ &\leq \left\| \frac{1}{B} \sum_{b=1}^B (\mu(h_{\theta_\ell}(x_i))_{b,c} - \mu(h_{\theta'_\ell}(x_i))_{b,c}) \right\| \\ &\leq \frac{1}{B} \sum_{b=1}^B \|\mu(h_{\theta_\ell}(x_i))_{b,c} - \mu(h_{\theta'_\ell}(x_i))_{b,c}\|, \end{aligned} \quad (37)$$

in which we used the triangle inequality. Therefore, we must establish Lipschitz continuity of $\mu(h_{\theta_\ell}(x_i))_{b,c}$. Using the definition of the function $\mu(\cdot)_{b,c}$ given in Eq. (2), we have that

$$\begin{aligned} &\|\mu(h_{\theta_\ell}(x_i))_{b,c} - \mu(h_{\theta'_\ell}(x_i))_{b,c}\| \\ &\leq \left\| \frac{1}{HW} \sum_{h=1}^H \sum_{w=1}^W (h_{\theta_\ell}(x_i)_{b,c,h,w} - h_{\theta'_\ell}(x_i)_{b,c,h,w}) \right\| \\ &\leq \frac{1}{HW} \sum_{h=1}^H \sum_{w=1}^W \|h_{\theta_\ell}(x_i)_{b,c,h,w} - h_{\theta'_\ell}(x_i)_{b,c,h,w}\| \\ &\leq \frac{1}{HW} \sum_{h=1}^H \sum_{w=1}^W D_{i,\ell} \|\theta - \theta'\| = D_{i,\ell} \|\theta - \theta'\|, \end{aligned} \quad (38)$$

where we used the triangle inequality first, then invoked Assumption 5.3-(a). Plugging the result of Eq. (38) back in Eq. (37), we obtain

$$\|\bar{\mu}_{\theta,\ell}(x_i)_c - \bar{\mu}_{\theta',\ell}(x_i)_c\| \leq \frac{1}{B} \sum_{b=1}^B D_{i,\ell} \|\theta - \theta'\| = D_{i,\ell} \|\theta - \theta'\|. \quad (39)$$

\square

PROOF. (b) Using the definition $\bar{\sigma}_{\theta,\ell}(x_i)_c = \frac{1}{B} \sum_{b=1}^B \sigma(h_{\theta_\ell}(x_i))_{b,c}$ given in Eq. (15), we have that

$$\begin{aligned} &\|\bar{\sigma}_{\theta,\ell}(x_i)_c - \bar{\sigma}_{\theta',\ell}(x_i)_c\| \\ &= \left\| \frac{1}{B} \sum_{b=1}^B (\sigma(h_{\theta_\ell}(x_i))_{b,c} - \sigma(h_{\theta'_\ell}(x_i))_{b,c}) \right\| \\ &\leq \frac{1}{B} \sum_{b=1}^B \|\sigma(h_{\theta_\ell}(x_i))_{b,c} - \sigma(h_{\theta'_\ell}(x_i))_{b,c}\|, \end{aligned} \quad (40)$$

in which we used the triangle inequality. Thus, we must establish Lipschitz continuity of $\sigma(h_{\theta_\ell}(x_i))_{b,c}$. Towards this, we first use the difference of squares rule to obtain

$$\begin{aligned} &\|\sigma(h_{\theta_\ell}(x_i))_{b,c} - \sigma(h_{\theta'_\ell}(x_i))_{b,c}\| \\ &= \frac{\|\sigma^2(h_{\theta_\ell}(x_i))_{b,c} - \sigma^2(h_{\theta'_\ell}(x_i))_{b,c}\|}{\|\sigma(h_{\theta_\ell}(x_i))_{b,c} + \sigma(h_{\theta'_\ell}(x_i))_{b,c}\|} \\ &\geq \frac{\|\sigma^2(h_{\theta_\ell}(x_i))_{b,c} - \sigma^2(h_{\theta'_\ell}(x_i))_{b,c}\|}{\min_{\theta_\ell, x_i} \{\|\sigma(h_{\theta_\ell}(x_i))_{b,c}\|\}} \\ &\geq \frac{1}{\gamma_{i,\ell}} \|\sigma^2(h_{\theta_\ell}(x_i))_{b,c} - \sigma^2(h_{\theta'_\ell}(x_i))_{b,c}\|, \end{aligned} \quad (41)$$

where we used the fact that $\sigma(\cdot)_{b,c} > 0$ is always non-negative, and then invoked Assumption 5.3-(c). Similar to before, we must establish Lipschitz continuity of $\sigma^2(h_{\theta_\ell}(x_i))_{b,c}$ to prove Eq. (41) (and in turn of Eq. (40)). Using the definition of the function $\sigma^2(\cdot)_{b,c}$ in Eq. (2), we have that

$$\begin{aligned} \sigma^2(h_{\theta_\ell}(x_i))_{b,c} &= \frac{1}{HW} \sum_{h=1}^H \sum_{w=1}^W (h_{\theta_\ell}(x_i)_{b,c,h,w} - \mu(h_{\theta_\ell}(x_i))_{b,c})^2 \\ &= \frac{1}{HW} \sum_{h=1}^H \sum_{w=1}^W h_{\theta_\ell}(x_i)_{b,c,h,w}^2 - \mu(h_{\theta_\ell}(x_i))_{b,c}^2. \end{aligned} \quad (42)$$

Thus, we can obtain the following for the last term in Eq. (41)

$$\begin{aligned} &\|\sigma^2(h_{\theta_\ell}(x_i))_{b,c} - \sigma^2(h_{\theta'_\ell}(x_i))_{b,c}\| \\ &= \left\| \frac{1}{HW} \sum_{h=1}^H \sum_{w=1}^W (h_{\theta_\ell}(x_i)_{b,c,h,w}^2 - h_{\theta'_\ell}(x_i)_{b,c,h,w}^2) \right. \\ &\quad \left. - (\mu(h_{\theta_\ell}(x_i))_{b,c}^2 - \mu(h_{\theta'_\ell}(x_i))_{b,c}^2) \right\| \\ &\leq \frac{1}{HW} \sum_{h=1}^H \sum_{w=1}^W \|h_{\theta_\ell}(x_i)_{b,c,h,w}^2 - h_{\theta'_\ell}(x_i)_{b,c,h,w}^2\| \\ &\quad + \|\mu(h_{\theta_\ell}(x_i))_{b,c}^2 - \mu(h_{\theta'_\ell}(x_i))_{b,c}^2\|, \end{aligned} \quad (43)$$

in which we used the triangle inequality. To bound Eq. (43), we focus on its constituents. We first have that

$$\begin{aligned} &\|h_{\theta_\ell}(x_i)_{b,c,h,w}^2 - h_{\theta'_\ell}(x_i)_{b,c,h,w}^2\| \\ &= \|h_{\theta_\ell}(x_i)_{b,c,h,w} + h_{\theta'_\ell}(x_i)_{b,c,h,w}\| \\ &\quad \|h_{\theta_\ell}(x_i)_{b,c,h,w} - h_{\theta'_\ell}(x_i)_{b,c,h,w}\| \\ &\leq 2 \max_{\theta_\ell, x_i} \{\|h_{\theta_\ell}(x_i)_{b,c,h,w}\|\} D_{i,\ell} \|\theta - \theta'\| = 2U_{i,\ell} D_{i,\ell} \|\theta - \theta'\|, \end{aligned} \quad (44)$$

where we used the difference of squares formula, and then invoked Assumption 5.3-(a) and 5.3-(b). For the second term in Eq. (43), we

have

$$\begin{aligned} & \|\mu(h_{\theta_\ell}(x_i))_{b,c}^2 - \mu(h_{\theta'_\ell}(x_i))_{b,c}^2\| \\ &= \|\mu(h_{\theta_\ell}(x_i))_{b,c} + \mu(h_{\theta'_\ell}(x_i))_{b,c}\| \\ & \quad \|\mu(h_{\theta_\ell}(x_i))_{b,c} - \mu(h_{\theta'_\ell}(x_i))_{b,c}\| \\ & \leq 2 \max_{\theta_\ell, x_i} \{\|\mu(h_{\theta_\ell}(x_i))_{b,c}\|\} D_{i,\ell} \|\theta - \theta'\| = 2U_{i,\ell} D_{i,\ell} \|\theta - \theta'\|, \end{aligned} \quad (45)$$

where we used the difference of squares formula, and then invoked the results of Lemma 5.4-(a) and Proposition 5.5-(a). Putting Eqs. (44) and (45) together and plugging them back in (43), and then we get

$$\begin{aligned} & \|\sigma^2(h_{\theta_\ell}(x_i))_{b,c} - \sigma^2(h_{\theta'_\ell}(x_i))_{b,c}\| \\ & \leq \frac{1}{HW} \sum_{h=1}^H \sum_{w=1}^W 2U_{i,\ell} D_{i,\ell} \|\theta - \theta'\| + 2U_{i,\ell} D_{i,\ell} \|\theta - \theta'\| \\ & = 4U_{i,\ell} D_{i,\ell} \|\theta - \theta'\|. \end{aligned} \quad (46)$$

Finally, we employ Eq. (46) in Eq. (41) followed by Eq. (40) to get

$$\begin{aligned} \|\bar{\sigma}_{\theta,\ell}(x_i)_c - \bar{\sigma}_{\theta',\ell}(x_i)_c\| & \leq \frac{1}{B} \sum_{b=1}^B \frac{4U_{i,\ell} D_{i,\ell}}{\gamma_{i,\ell}} \|\theta - \theta'\| \\ & = \frac{4U_{i,\ell} D_{i,\ell}}{\gamma_{i,\ell}} \|\theta - \theta'\|. \end{aligned} \quad (47)$$

□

PROOF. (c) Using the definition $\Sigma_{\mu,\theta,\ell}^2(x_i)_c = \Sigma_{\mu}^2(h_{\theta_\ell}(x_i))_c$ given in Eq. (15) and the definition of the function $\Sigma_{\mu}^2(\cdot)_c$ in Eq. (3), we have that

$$\begin{aligned} \Sigma_{\mu,\theta,\ell}^2(x_i)_c &= \frac{1}{B} \sum_{b=1}^B (\mu(h_{\theta_\ell}(x_i))_{b,c} - \mathbb{E}_b[\mu(h_{\theta_\ell}(x_i))_{b,c}])^2 \\ &= \frac{1}{B} \sum_{b=1}^B \mu(h_{\theta_\ell}(x_i))_{b,c}^2 - \bar{\mu}_{\theta,\ell}(x_i)_c^2, \end{aligned} \quad (48)$$

where we used the definition of $\bar{\mu}_{\theta,\ell}(x_i)_c$ from Eq. (15). Consequently, we can obtain the bound

$$\begin{aligned} & \|\Sigma_{\mu,\theta,\ell}^2(x_i)_c - \Sigma_{\mu,\theta',\ell}^2(x_i)_c\| \\ &= \left\| \frac{1}{B} \sum_{b=1}^B (\mu(h_{\theta_\ell}(x_i))_{b,c}^2 - \mu(h_{\theta'_\ell}(x_i))_{b,c}^2) \right. \\ & \quad \left. - (\bar{\mu}_{\theta,\ell}(x_i)_c^2 - \bar{\mu}_{\theta',\ell}(x_i)_c^2) \right\| \\ & \leq \frac{1}{B} \sum_{b=1}^B \|\mu(h_{\theta_\ell}(x_i))_{b,c}^2 - \mu(h_{\theta'_\ell}(x_i))_{b,c}^2\| \\ & \quad + \|\bar{\mu}_{\theta,\ell}(x_i)_c^2 - \bar{\mu}_{\theta',\ell}(x_i)_c^2\|, \end{aligned} \quad (49)$$

in which we used the triangle inequality. We have obtained a bound for the first term of Eq. (49) in Eq. (45), and we focus on the second term next. We have that

$$\begin{aligned} & \|\bar{\mu}_{\theta,\ell}(x_i)_c^2 - \bar{\mu}_{\theta',\ell}(x_i)_c^2\| \\ &= \|\bar{\mu}_{\theta,\ell}(x_i)_c + \bar{\mu}_{\theta',\ell}(x_i)_c\| \|\bar{\mu}_{\theta,\ell}(x_i)_c - \bar{\mu}_{\theta',\ell}(x_i)_c\| \\ & \leq 2 \max_{\theta, l, x_i} \{\|\bar{\mu}_{\theta,\ell}(x_i)_c\|\} D_{i,\ell} \|\theta - \theta'\| = 2U_{i,\ell} D_{i,\ell} \|\theta - \theta'\|, \end{aligned} \quad (50)$$

where we used the difference of squares law, and then invoke the results of Lemma 5.4-(c) and Proposition 5.5-(a), respectively. To conclude the proof, we plug back Eqs. (50) and (45) back in Eq. (49) to get

$$\begin{aligned} & \|\Sigma_{\mu,\theta,\ell}^2(x_i)_c - \Sigma_{\mu,\theta',\ell}^2(x_i)_c\| \\ & \leq \frac{1}{B} \sum_{b=1}^B 2U_{i,\ell} D_{i,\ell} \|\theta - \theta'\| + 2U_{i,\ell} D_{i,\ell} \|\theta - \theta'\| \\ & = 4U_{i,\ell} D_{i,\ell} \|\theta - \theta'\|. \end{aligned} \quad (51)$$

□

PROOF. (d) Using the definition $\Sigma_{\sigma,\theta,\ell}^2(x_i)_c = \Sigma_{\sigma}^2(h_{\theta_\ell}(x_i))_c$ given in Eq. (15) and the definition of the function $\Sigma_{\sigma}^2(\cdot)_c$ in Eq. (3), we have that

$$\begin{aligned} \Sigma_{\sigma,\theta,\ell}^2(x_i)_c &= \frac{1}{B} \sum_{b=1}^B (\sigma(h_{\theta_\ell}(x_i))_{b,c} - \mathbb{E}_b[\sigma(h_{\theta_\ell}(x_i))_{b,c}])^2 \\ &= \frac{1}{B} \sum_{b=1}^B \sigma(h_{\theta_\ell}(x_i))_{b,c}^2 - \bar{\sigma}_{\theta,\ell}^2(x_i)_c, \end{aligned} \quad (52)$$

where we used the definition of $\bar{\sigma}_{\theta,\ell}^2(x_i)_c$ from Eq. (15). Hence, we can obtain the bound

$$\begin{aligned} & \|\Sigma_{\sigma,\theta,\ell}^2(x_i)_c - \Sigma_{\sigma,\theta',\ell}^2(x_i)_c\| \\ &= \left\| \frac{1}{B} \sum_{b=1}^B (\sigma(h_{\theta_\ell}(x_i))_{b,c}^2 - \sigma(h_{\theta'_\ell}(x_i))_{b,c}^2) \right. \\ & \quad \left. - (\bar{\sigma}_{\theta,\ell}^2(x_i)_c - \bar{\sigma}_{\theta',\ell}^2(x_i)_c) \right\| \\ & \leq \frac{1}{B} \sum_{b=1}^B \|\sigma(h_{\theta_\ell}(x_i))_{b,c}^2 - \sigma(h_{\theta'_\ell}(x_i))_{b,c}^2\| \\ & \quad + \|\bar{\sigma}_{\theta,\ell}^2(x_i)_c - \bar{\sigma}_{\theta',\ell}^2(x_i)_c\|, \end{aligned} \quad (53)$$

in which we used the triangle inequality. We have obtained bounds for the first term of Eq. (53) in Eq. (46), and we focus on the second term next. We have that

$$\begin{aligned} & \|\bar{\sigma}_{\theta,\ell}(x_i)_c^2 - \bar{\sigma}_{\theta',\ell}(x_i)_c^2\| \\ &= \|\bar{\sigma}_{\theta,\ell}(x_i)_c + \bar{\sigma}_{\theta',\ell}(x_i)_c\| \|\bar{\sigma}_{\theta,\ell}(x_i)_c - \bar{\sigma}_{\theta',\ell}(x_i)_c\| \\ & \leq 2 \max_{\theta, l, x_i} \{\|\bar{\sigma}_{\theta,\ell}(x_i)_c\|\} \frac{4U_{i,\ell} D_{i,\ell}}{\gamma_{i,\ell}} \|\theta - \theta'\| = \frac{8\sqrt{2}U_{i,\ell}^2 D_{i,\ell}}{\gamma_{i,\ell}} \|\theta - \theta'\|, \end{aligned} \quad (54)$$

where we used the difference of squares law, and then invoke the results of Lemma 5.4-(d) and Proposition 5.5-(b), respectively. To conclude the proof, we plug back Eqs. (54) and (46) back in Eq. (49) to get

$$\begin{aligned} & \|\Sigma_{\sigma,\theta,\ell}^2(x_i)_c - \Sigma_{\sigma,\theta',\ell}^2(x_i)_c\| \\ & \leq \frac{1}{B} \sum_{b=1}^B 4U_{i,\ell} D_{i,\ell} \|\theta - \theta'\| + \frac{8\sqrt{2}U_{i,\ell}^2 D_{i,\ell}}{\gamma_{i,\ell}} \|\theta - \theta'\| \\ & = 4U_{i,\ell} D_{i,\ell} \left(1 + \frac{2\sqrt{2}U_{i,\ell}}{\gamma_{i,\ell}}\right) \|\theta - \theta'\|. \end{aligned} \quad (55)$$

□

D Proof of Lemma 5.6

PROOF. (a) With the bounds for all 4 individual style statistics of each device $i \in \mathcal{M}$ at a given layer/block $\ell = \{1, \dots, L\}$ derived in Proposition 5.5, we move on to analyze the Lipschitz continuity of $\psi_{\theta,\ell}(x_i) = \left[\bar{\mu}_{\theta,\ell}(x_i) \quad \bar{\sigma}_{\theta,\ell}(x_i) \quad \Sigma_{\mu,\theta,\ell}^2(x_i) \quad \Sigma_{\sigma,\theta,\ell}^2(x_i) \right]^T$, which is a vector concatenating all of them for a single client i at a single layer ℓ . We have

$$\begin{aligned} & \|\psi_{\theta,\ell}(x_i) - \psi_{\theta',\ell}(x_i)\| \\ & \leq \|\bar{\mu}_{\theta,\ell}(x_i) - \bar{\mu}_{\theta',\ell}(x_i)\| + \|\bar{\sigma}_{\theta,\ell}(x_i) - \bar{\sigma}_{\theta',\ell}(x_i)\| \\ & \quad + \|\Sigma_{\mu,\theta,\ell}^2(x_i) - \Sigma_{\mu,\theta',\ell}^2(x_i)\| + \|\Sigma_{\sigma,\theta,\ell}^2(x_i) - \Sigma_{\sigma,\theta',\ell}^2(x_i)\| \\ & \leq \left(D_{i,\ell} + \frac{4U_{i,\ell}D_{i,\ell}}{\gamma_{i,\ell}} + 4U_{i,\ell}D_{i,\ell} + 4U_{i,\ell}D_{i,\ell} \left(1 + \frac{2\sqrt{2}U_{i,\ell}}{\gamma_{i,\ell}} \right) \right) \|\theta - \theta'\| \\ & = \left(1 + 4U_{i,\ell} \left(1/\gamma_{i,\ell} + 2 + (2\sqrt{2}U_{i,\ell})/\gamma_{i,\ell} \right) \right) D_{i,\ell} \|\theta - \theta'\|, \end{aligned} \quad (56)$$

in which we used the triangle inequality. Next, we focus on $\psi_{\theta}(x_i) = \left[\psi_{\theta,1}(x_i) \quad \dots \quad \psi_{\theta,L}(x_i) \right]^T$, which is a vector concatenating the style statistics across all the layers of the CNN for a given client $i \in \mathcal{M}$. We have that

$$\begin{aligned} \|\psi_{\theta}(x_i) - \psi_{\theta'}(x_i)\| & \leq \sum_{\ell=1}^L \|\psi_{\theta,\ell}(x_i) - \psi_{\theta',\ell}(x_i)\| \\ & \leq L \left(1 + 4U_i \left(1/\gamma_i + 2 + (2\sqrt{2}U_i)/\gamma_i \right) \right) D_i \|\theta - \theta'\|, \end{aligned} \quad (57)$$

in which we used the triangle inequality. Finally, the Lipschitzness of $\Psi_{\theta}(X) = \left[\psi_{\theta}(x_1) \quad \dots \quad \psi_{\theta}(x_m) \right]^T$ follows similarly as

$$\begin{aligned} \|\Psi_{\theta}(X) - \Psi_{\theta'}(X)\| & \leq \sum_{i=1}^m \|\psi_{\theta}(x_i) - \psi_{\theta'}(x_i)\| \\ & \leq mL \left(1 + 4U \left(1/\gamma + 2 + (2\sqrt{2}U)/\gamma \right) \right) D \|\theta - \theta'\|, \end{aligned} \quad (58)$$

in which we used the triangle inequality, and m is the total number of devices in the decentralized network. Noting that $\Psi_{\theta_i}(X) \subset \Psi_{\theta}(X)$, we thus have that

$$\|\Psi_{\theta_i}(X) - \Psi_{\theta',i}(X)\| \leq mL \left(1 + 4U \left(1/\gamma + 2 + (2\sqrt{2}U)/\gamma \right) \right) D \|\theta - \theta'\|. \quad (59)$$

Plugging the last equation above into Assumption 5.1, we obtain

$$\begin{aligned} & \|\nabla F_i(\theta, \Psi_{\theta_i}(X)) - \nabla F_i(\theta', \Psi_{\theta',i}(X))\| \\ & \leq \beta_{\theta,i} \|\theta - \theta'\| + \beta_{\Psi,i} \|\Psi_{\theta_i}(X) - \Psi_{\theta',i}(X)\| \\ & \leq \left[\beta_{\theta,i} + mL \left(1 + 4U \left(1/\gamma + 2 + (2\sqrt{2}U)/\gamma \right) \right) D\beta_{\Psi,i} \right] \|\theta - \theta'\|. \end{aligned} \quad (60)$$

□

PROOF. (b) Using the definition of the global loss function given in Eq. (20) and the result of Lemma 5.6-(a), we have

$$\begin{aligned} & \|F(\theta) - F(\theta')\| \\ & \leq \frac{1}{m} \sum_{i=1}^m \mathbb{E}_{\{(x_j, y_j) \sim \mathbb{P}_{D_j}\}_{j \in \mathcal{M}}} \left[\|F_i(\theta, \Psi_{\theta_i}(X)) - F_i(\theta', \Psi_{\theta',i}(X))\| \right] \\ & \leq \frac{1}{m} \sum_{i=1}^m \mathbb{E}_{\{(x_j, y_j) \sim \mathbb{P}_{D_j}\}_{j \in \mathcal{M}}} \left[\beta_i \|\theta - \theta'\| \right] \\ & = \left(\frac{1}{m} \sum_{i=1}^m \beta_i \right) \|\theta - \theta'\|. \end{aligned} \quad (61)$$

in which we used the triangle inequality first, and then Jensen's inequality in the form $\|\mathbb{E}[\cdot]\| \leq \mathbb{E}[\|\cdot\|]$. □

E Proof of Theorem 5.7

PROOF. With the univariate smoothness of local loss functions being established in Lemma 5.6-(a), we can utilize the theoretical results of well-known papers on decentralized optimization to provide convergence guarantees for StyleDDG. The proof is concluded using the Theorems in [17, 43]. □

Received 6 April 2025